Nuclear Physics B136 (1978) 1–76

A PARAMETRIZATION OF THE PROPERTIES OF QUARK JETS *

R.D. FIELD and R.P. FEYNMAN
California Institute of Technology, Pasadena, California 91125, USA

Received 11 October 1977

A model is analyzed that provides a parametrization of the properties of the jet of mesons generated by a fast outgoing quark. It is assumed that the meson that contains the original quark leaves momentum and flavor to a remaining jet in which the particles are distributed (except for scaling of the energy and possible changes of flavor) like those of the original jet. One function, the probability $f(\eta)$ that the remaining jet has a fraction η of the momentum of the original jet, is chosen (as a parabola) so the final distribution of charged hadrons agrees with data from lepton experiments. All the properties of quark jets are determined from $f(\eta)$ and three parameters; the degree that SU(3) is broken in the formation of new quark-antiquark pairs ($\bar{s}s$ is taken as half as likely as $\bar{u}u$), the spin nature of the primary mesons (assumed to be vector and pseudoscalar with equal probability), and the mean transverse momentum given to these primary mesons. Monte Carlo methods are used to generate typical jets. Analytic approximations are also given. Many features of quark jets are examined. The distribution of momentum of various hadrons $D_q^h(z)$, the properties of the hadrons of largest momentum in the jet, correlations, rapidity-gap distributions, distribution of charge and of transverse momentum are some of the subjects discussed. The appearance of the jets to an instrument sensitive only to particles above some minimum momentum is also described. Although the model is probably not a true description of the physical mechanism responsible for quark jets, many predictions of the model seem quite reasonable, possibly much like real quark jets (except that the possibility of the emission of baryons is disregarded). The purpose of this work is to provide a model useful in the design of experiments in which quark jets may be observed, and further to provide a standard to facilitate the comparison of lepton-generated jets with the high-$p_\perp$ jets found in hadron collisions.

1. Introduction

Recent data from ISR [1,2] and Fermilab [3] indicate that the "jets" observed in large-$p_\perp$ hadron-hadron collisions are similar to those in processes initiated by leptons (i.e., e^+e^-, ep, and νp processes). The "jets" observed in both cases are thought to arise from quarks that fragment or cascade into a collection of hadrons moving in roughly the direction of the original quark.

* Work supported in part by the US Energy Research and Development Administration under Contract No. EY76-C-03-0068.

The experimental verification of this should proceed simultaneously in two directions. First, the detailed properties of the jets produced in lepton reactions must be examined. (Incidentally, we must confirm *via* charge properties, etc., that these jets could actually arise from quarks.) Secondly, the hadron-initiated large-$p_\perp$ jets must be compared in great detail to the lepton jets to determine if they are actually identical. (Some theorists believe that gluon jets will be produced at large $p_\perp$ in hadron-hadron collisions in addition to quark jets.) At the present time there is little data of either kind. However, hadron "jet trigger" experiments are proceeding or are planned. There is no comprehensive theory of the details of the jet structure that we should expect to observe. So, it will be difficult to know in, say, a hadron experiment what data to collect and how to summarize it so that it will be useful to compare to some future lepton experiment which will probably not measure precisely the same thing. We thought it might prove useful to have some easy-to-analyze "standard" jet structure to compare to. Thus, a hadron experiment could say "the real jets differ from the 'standard' in such and such a way", and the lepton experiment could then see whether they deviated from the same 'standard' in a similar way.

In a previous paper [4] (hereafter called FF1), we used limited experimental data aided by some theoretical ideas to suggest parametrizations for the functions $D_q^h(z)$, the mean number of hadrons of type h and momentum fraction z (per dz) in a jet initiated by a quark of flavor q with high momentum. The model presented here provides a new, much simpler, parametrization for these functions, making only negligible changes for those functions that were determined by experiment and otherwise in agreement with all the theoretical ideas in FF1.

A virtue of the new model is that it gives detailed answers to many other questions such as the number of correlated pairs of hadrons h_1, h_2 at z_1 and z_2, or the distributions of momentum gaps containing no hadrons, or the probability of observing various total jet charges, etc. In addition, one can ask for the probability that a quark of large momentum fragments so that the sum of the fractional momenta z_1, z_2, ... of all those hadrons with $z_i > z_{\min}$ is z. The latter is useful in analyzing "jet trigger" experiments. In this type of experiment, one triggers on a collection of particles that sum to give a large $p_\perp$. It is experimentally very difficult to define a "jet". One can never be sure that all the low-momentum particles from the quark are included *or* that one has not included some extra low-$p_\perp$ particles from the background of particles moving in the beam or target jets and not properly belonging to the transverse jet. These experiments would be much cleaner if one sets a threshold $p_{\perp 0}$, say, 500 MeV, for the transverse momenta of the particles whose total momentum makes up the trigger (so $z_{\min} = p_{\perp 0}/p_\perp(\text{quark})$).

We generate typical jets using Monte Carlo methods but provide an analytic approximation for the convenience of the reader. The predictions of the model are reasonable enough physically that we expect it may be close enough to reality to be useful in designing future experiments and to serve as a reasonable approximation to compare to data. We do not think of the model as a sound physical theory, and dis-

cuss why in a later section. Also, as worked out here, the model does not include baryons. We must imagine the jets to contain only mesons because we have so little knowledge at present of what baryons to expect and the character of the model does not make a clear suggestion. It also makes no clear suggestion of what correlations in transverse momentum of the hadrons to expect. We have added an additional assumption to determine this which seems reasonable to us but may be far from the physical situation. Some of the features of the transverse-momentum distributions are, however, strongly affected by the fact that the particles observed are often products of decays of higher resonances. These effects are not dependent on the details of our jet model and should be important also in analyzing the beam and target jets in ordinary inelastic hadron-hadron collisions.

Our quark-jet model involves one arbitrary function, the probability $f(\eta)$ that the hadron containing the original quark leaves the remaining jet a fraction η of its momentum. This ultimately determines the momentum distribution of hadrons. We have found that taking $f(\eta)$ to be a parabola with one adjustable parameter results in an adequate fit to the distribution of charged hadrons, $D_q^{h^+}(z) + D_q^{h^-}(z)$, observed in lepton experiments. All the properties of quark jets are then determined from $f(\eta)$ and three additional parameters; the degree that SU(3) is broken in the formation of new quark-antiquark pairs ($s\bar{s}$ is taken as half as likely as $\bar{u}u$), the spin of the primary mesons (assumed to be vector and pseudoscalar with equal probability), and the mean transverse momentum given to these primary mesons. This later parameter is determined by requiring that the final hadrons (after decay) have a mean transverse momentum of about 330 MeV.

2. The model

2.1. *The ansatz*

We assume that quark jets can be analyzed on the basis of a recursive principle. The ansatz is based on the idea that a quark of type "a" coming out at some momentum W_0 in the z direction creates a color field in which new quark-antiquark pairs are produced. Quark "a" then combines with an antiquark, say "$\bar{b}$", from the new pair $\bar{b}b$ to form a meson "$a\bar{b}$" leaving the remaining quark "b" to combine with further antiquarks. The "meson" $a\bar{b}$ may be directly observed as a pseudoscalar meson, or it may be a vector or higher-spin unstable resonance which subsequently decays into the observed mesons. To avoid complicating the ideas, we will call "$a\bar{b}$" the "primary" meson state and shall discuss secondary decay processes later. A "hierarchy" of primary mesons is formed of which $a\bar{b}$ is first in "rank", $b\bar{c}$ is second in rank, $c\bar{d}$ is third in rank, etc., as shown in fig. 1. (The "rank" in "hierarchy" should *not* be confused with order in momentum, but only order in the flavor relationships. The rank-2 primary meson may sometimes obtain a larger momentum than the rank-1 primary meson.)

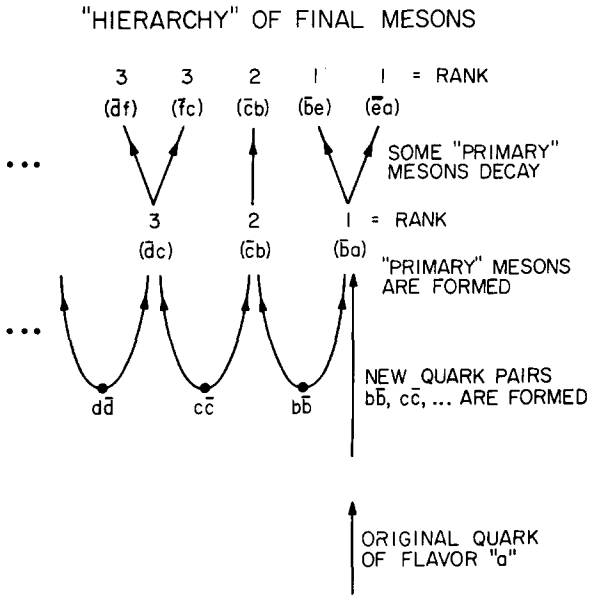

Fig. 1. Illustration of the "hierarchy" structure of the final mesons produced when a quark of type "a" fragments into hadrons. New quark pairs $b\bar{b}$, $c\bar{c}$, etc., are produced and "primary" mesons are formed. The "primary" meson $\bar{b}a$ that contains the original quark is said to have "rank" one and primary meson $\bar{c}b$ rank two, etc. Finally, some of the primary mesons decay and we assign all the decay products to have the rank of the parent. The order in "hierarchy" is *not* the same as order in momentum or rapidity.

The "chain decay" ansatz * assumes that, if the rank-1 primary meson carries away a momentum ξ_1 (from a quark jet of type "a" and momentum W_0) the remaining cascade starts with a quark of type "b" with momentum $W_1 = W_0 - \xi_1$ and the remaining hadrons are distributed in exactly the same way as the hadrons which come from a jet originated by a quark of type "b" with momentum W_1. It is further assumed that for very high momenta, all distributions scale so that they depend only on ratios of the hadron momenta to the quark momenta. Given these assumptions, complete knowledge of the structure of a quark jet is determined by one unknown function $f(\eta)$ and three parameters describing flavor, primary meson spin, and transverse momentum to be discussed later. The function $f(\eta)$ is defined by

$f(\eta)\, d\eta$ = the probability that the first hierarchy (rank-1) primary meson *leaves* the fraction of momentum η to the remaining cascade, (2.1)

* We believe this recursive principle was first suggested by Krywicki and Petersson [6] and by Finkelstein and Peccei [7] in an analysis of proton-proton collisions.

and is normalized so that

$$\int_0^1 f(\eta)\, d\eta = 1 \,. \tag{2.2}$$

The rank-1 primary meson (with momentum fraction $z_1 = \xi_1/W_0$) contains the original quark "a" (see fig. 1) and $\eta = 1 - z_1$. Thus for an initial quark with momentum W_0, the probability that the first-hierarchy primary meson has momentum ξ_1 in $d\xi_1$ is $f(1 - \xi_1/W_0)\, d\xi_1/W_0$ and the probability that the rank-2 primary meson has momentum ξ_2 in $d\xi_2$ is $f(1 - \xi_2/W_1)\, d\xi_2/W_1$, where $W_1 = W_0 - \xi_1$, etc. The probability that we have a hierarchy sequence of primary mesons with the kth having momentum ξ_k in $d\xi_k$ is

$$\text{Prob}(\xi_1, \xi_2, ..., \xi_k)\, d\xi_1\, d\xi_2 \ldots d\xi_k \ldots = \prod_{i=1}^{\infty} f(\eta_i)\, d\eta_i \,, \tag{2.3}$$

where $\eta_i = W_i/W_{i-1}$ with $\xi_i = W_{i-1} - W_i$. That is, $\eta_i = 1 - \xi_i/W_{i-1}$ and $d\eta_i$ is to be replaced by $d\xi_i/W_i$ with $W_i = W_0 - \Sigma_{k=1}^{i} \xi_k$.

2.2. *Single-particle decay distribution $F(z)$*

The above ansatz leads to an obvious and simple Monte Carlo calculation of a jet as well as to a straightforward recursive integral equation. For example, if we define a single-particle distribution in the quark jet as

$F(z)\, dz$ = the probability of finding any primary meson (independent of hierarchy) with fractional momentum z within dz in a quark jet, (2.4)

then $F(z)$ must satisfy the following integral equation (take $W_0 = 1$)

$$F(z) = f(1 - z) + \int_z^1 f(\eta) F(z/\eta)\, d\eta/\eta \,, \tag{2.5}$$

where the limits are automatic since we define $f(1 - z) = 0$ and $F(z) = 0$ for $z > 1$ or $z < 0$. Eq. (2.5) arises because the primary meson might be the first in rank (with probability $f(1 - z)\, dz$) or if not, then the first-rank primary meson has left a momentum fraction η with probability $f(\eta)\, d\eta$, and in this remaining cascade the probability to find z in dz is $F(z/\eta)\, dz/\eta$ by the scaling principle. Dividing out the dz leaves eq. (2.5).

An integral equation for $F(z)$ given $f(\eta)$ as (2.5) involves only differences in rapidity ($Y_z = -\ln z$) * and hence can easily be analyzed by a Fourier transform

* In this paper, we will use the word rapidity to refer either to the "z rapidity" given by $Y_z = -\ln z$ in (3.4) *or* the true rapidity given by eq. (3.5). Usually the difference between the two will not be important; however, when it is, we label the former by Y_z and the latter by Y.

in rapidity, or equivalently by taking moments in z. If we define

$$M(r) = \int_0^1 z^r F(z)\, dz\,, \tag{2.6a}$$

$$C(r) = \int_0^1 \eta^r f(\eta)\, d\eta\,, \tag{2.6b}$$

then eq. (2.5) takes the form

$$M(r) = A(r) + C(r)\, M(r) \tag{2.7a}$$

or

$$M(r) = A(r)/(1 - C(r))\,, \tag{2.7b}$$

where

$$A(r) = \int_0^1 z^r f(1 - z)\, dz\,. \tag{2.7c}$$

The function $A(r)$ is, of course, related to $C(r)$ for they are determined by the same function, but the point we wish to make here is more general. The integral kernel of (2.5) can be inverted algebraically in moment space as

$$1/(1 - C(r)) = 1 + C(r)/(1 - C(r))\,. \tag{2.7d}$$

Thus an equation of the form

$$\phi(z) = a(z) + \int f(\eta)\, \phi(z/\eta)\, d\eta/\eta \tag{2.8a}$$

can be inverted to give

$$\phi(z) = a(z) + \int g(\eta)\, a(z/\eta)\, d\eta/\eta\,, \tag{2.8b}$$

where

$$\int \eta^r g(\eta)\, d\eta = C(r)/(1 - C(r))\,. \tag{2.8c}$$

For example, (2.5) is solved by

$$F(z) = f(1 - z) + \int_z^1 g(\eta)\, f(1 - z/\eta)\, d\eta/\eta\,, \tag{2.9}$$

which can be interpreted in the following way. If a particle is found at z, either it is a first-rank primary meson or else the particles of lower rank have left a momentum

η, and it is the first of those remaining (i.e., $f(1-z/\eta)\,dz/\eta$). That is, $g(\eta)\,d\eta$ has the significance of being the probability that all the primary mesons of lower rank than a given particle have left momentum fraction η of the original momentum of the jet.

The probability normalization of $f(\eta)$ given by (2.2) means that $C(0) = 1$. Then from eq. (2.5) (or (2.7b) since $A(1) = 1 - C(1)$), one finds that the total momentum of all the primary mesons in the quark jet, $M(1)$, is unity (i.e., equal to the original quark momentum). Namely,

$$\int_0^1 zF(z)\,dz = 1\ . \tag{2.10}$$

Another important point is that for small z, eq. (2.5) implies that $F(z)$ has the expected $R\,dz/z$ behavior (R = constant). This represents a uniform distribution in rapidity, $Y_z = -\ln z$. We see from (2.7b) that $M(r)$ diverges as $r \to 0$, since $C(0) = 1$, as R/r where

$$1/R = -dC(r)/dr|_{r=0}\ , \tag{2.11a}$$

or

$$1/R = -\int_0^1 \ln \eta f(\eta)\,d\eta\ . \tag{2.11b}$$

For small r, the integral (2.6a) is dominated by small z if $F(z)$ is R/z and is R/r. This may also be understood as follows. Since rapidity Y_z is $-\ln z$, $1/R$ from (2.11b) is the mean loss of rapidity, $\ln \eta$, per primary meson. Thus, deep in the cascade we must have R primary mesons per unit of rapidity $dY_z = dz/z$. For small η, in the plateau, $g(\eta)$ in eq. (2.8c) is given by $g(\eta) = R/\eta$.

2.3. *Double-decay distribution* $F_2(z_1, z_2)$

Suppose we want the probability of finding two primary mesons, one at z_1, the other at z_2, regardless of their rank in hierarchy. First, we define the function $F_2(z_1, z_2)$ by

$$F_2(z_1, z_2)\,dz_1\,dz_2 = \text{the probability of finding two primary mesons, one at } z_1 \text{ of any rank and one at } z_2\text{, but of higher rank than the one at } z_1\ . \tag{2.12}$$

We can immediately write the integral equation

$$F_2(z_1, z_2) = f(1-z_1)\,F(z_2/(1-z_1))/(1-z_1) + \int f(\eta)\,F_2(z_1/\eta, z_2/\eta)\,d\eta/\eta^2\ . \tag{2.13}$$

The first term arises because z_1 might be the first-rank primary meson (probability

$f(1-z_1)\mathrm{d}z_1)$, and z_2 any primary meson in the following cascade (of total momentum $1-z_1$) and hence with probability $F(z_2/(1-z_1))\mathrm{d}z_2/(1-z_1)$. The second term arises if z_1 is not of rank one. The rank-one primary meson leaves the others with momentum η with probability $f(\eta)\mathrm{d}\eta$ and then we find z_1, z_2 with scaled probability $F_2(z_1/\eta, z_2/\eta)\,\mathrm{d}z_1/\eta\,\mathrm{d}z_2/\eta$. Eq. (2.13) can be solved by the techniques discussed in subsect. 2.2, whereupon one gets

$$F_2(z_1, z_2) = f(1-z_1)F(z_2/(1-z_1))/(1-z_1) + \int_{z_1+z_2}^{1} g(\eta)\, f(1-z_1/\eta)\, F(z_2/(\eta-z_1))\, \mathrm{d}\eta/(\eta(\eta-z_1)) \,. \tag{2.14}$$

The complete double-fragmentation function, where the meson at z_2 may be either of higher or lower rank than that at z_1, is then given by

$$\tilde{F}_2(z_1, z_2) = F_2(z_1, z_2) + F_2(z_2, z_1) \,. \tag{2.15}$$

2.4. Choosing the form of $f(\eta)$

A form which makes the solution of the integral equation (2.5) the simplest is a power of η,

$$f(\eta) = (d+1)\eta^d \,. \tag{2.16}$$

In this case

$$C(r) = (d+1)/(r+d+1) \tag{2.17a}$$

or

$$C(r)/(1-C(r)) = (d+1)/r \,, \tag{2.17b}$$

so that

$$g(\eta) = (d+1)/\eta \,, \tag{2.18a}$$

and hence

$$zF(z) = (d+1)(1-z)^d \,. \tag{2.18b}$$

This means that

$$zF(z) = f(1-z) \,, \tag{2.18c}$$

which serves as a rather rough approximation for other forms of $f(\eta)$. This power form for $f(\eta)$ leads to a double-decay function of the form

$$F_2(z_1, z_2)\,\mathrm{d}z_1\,\mathrm{d}z_2 = f(1-z_1-z_2)\frac{\mathrm{d}z_1}{z_1}\,\frac{\mathrm{d}z_2}{z_1+z_2} \,, \tag{2.19a}$$

or disregarding order of rank,

$$\widetilde{F}_2(z_1, z_2) = f(1 - z_1 - z_2)/z_1 z_2 \,, \tag{2.19b}$$

which can also serve as a rough approximation for other choices of $f(\eta)$ *. The inclusive probability to find N mesons with momenta $z_1, z_2, \ldots z_N$ is

$$\widetilde{F}_N(z_1, z_2. \ldots z_N)\, dz_1 \ldots dz_N = (d+1)^{N+1} (1 - \sum_{i=1}^{N} z_i)^d \prod_{i=1}^{N} \frac{dz_i}{z_i} \,. \tag{2.20}$$

This is the manner in which mesons are distributed in the one-dimensional field-theory model of Casher, Kogut and Susskind [10]. In fact, it results simply from the assumption of particles produced independently at random having an *a priori* probability β to exist and then to be distributed uniformly in two-dimensional relativistic phase space (i.e., uniformly in rapidity, dz/z). The total energy and momentum must, however, be that of the jet ($\beta = d + 1$).

Although the forms of (2.16) and (2.18b) are simple and easy to interpret, they do not agree with the assumption we used in FF1, that the probability of finding mesons in dz approaches a constant as $z \to 1$. Eq. (2.5) has the property that $F(z)$ approaches $f(1-z)$ as z becomes large. The mesons at large z almost surely contain the original quark and at $z = 1$, the meson must contain the original quark. Thus in order for $F(z)$ to approach a constant as $z \to 1$, we must require that $f(\eta)$ approach a constant as $\eta \to 0$, something that the form (2.16) does not do. A function that leads to results similar to those found in FF1 is simply (2.16) plus a small constant. We take

$$f(\eta) = 1 - a + 3a\eta^2 \,, \tag{2.21}$$

where the parameter a and the power, $d = 2$, are chosen by comparing $F(z)$ to experiment. (Actually we compare the charged-particle distribution, $D_q^{h^+}(z) + D_q^{h^-}(z)$, to data.) The form (2.21) gives

$$C(r) = (1-a)/(r+1) + 3a/(r+3) \,, \tag{2.22a}$$

so that using (2.8c) we find

$$g(\eta) = (3/\eta + 4a(1-a)\eta^{2-2a})/(3-2a) \,, \tag{2.22b}$$

and (2.8d) yields

$$\begin{aligned} zF(z) = {} & 3/(3-2a) \\ & + 3az^2/(2a-1) \\ & + 2a(2a^2 - 3a - 2)z^{3-2a}/((3-2a)(2a-1)) \,. \end{aligned} \tag{2.23}$$

As we will see later after discussing flavor, if we interpret all primary mesons as

* Eq. (2.19b) with $f(\eta) = 2\eta$ was used by Bjorken in ref. [8] to estimate the large-$p_\perp$ $\pi^0\pi^0$ cross section in pp collisions and by Ellis, Jacob and Landshoff in ref. [9] to estimate same side large-$p_\perp$ correlations in pp collisions.

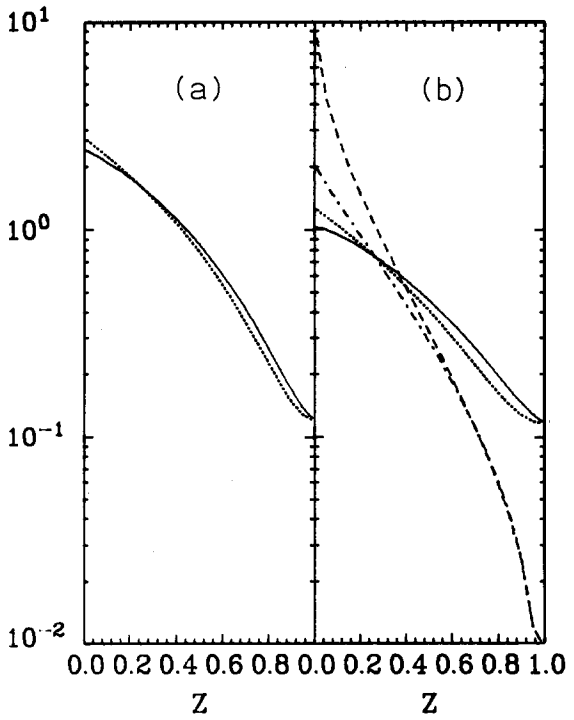

Fig. 2. (a) (left) The probability of finding the first-rank meson at z (in dz), $f(1-z)$ [---], and the probability of finding any hadron at z (times z), $zF(z)$ [——], given by eqs. (2.21) and (2.23), respectively, with $a = 0.88$, $\alpha_{ps} = 1$, $\alpha_v = 0$. (b) (right) The functions $\alpha_{ps} f(1-z)$ and $\alpha_{ps} zF(z)$ given by eqs. (2.21) and (2.23) with $a = 0.77$ together with the distribution of secondary mesons, $\alpha_v \hat{f}(1-z)$ and $\alpha_v z\hat{F}(z)$, from parents distributed according to (2.21) and (2.23), where $\alpha_{ps} = \alpha_v = 0.5$ and where we have used the parent-daughter relation in (2.54). —— $\alpha_{ps} zF(z)$; ..... $\alpha_{ps} f(1-z)$; $-\cdot-\cdot$ $\alpha_v z\hat{F}(z)$; $- - -$ $\alpha_v \hat{f}(1-z)$.

pseudoscalar mesons with no secondary decays then by comparing $D_q^{h^+}(z) + D_q^{h^-}(z)$ with data and with the results of FF1, we find that $a = 0.88$ gives a good fit. Fig. 2a shows $zF(z)$ and $f(1-z)$ for this case. We see that the relationship (2.18c) is still approximately valid.

2.5. *Including flavor*

Next we examine the question of the flavor u, d, s, $\bar{u}$, $\bar{d}$, and $\bar{s}$ of the quarks and hence the isospin and strangeness of the primary mesons. We call the isospin and strangeness properties the "flavor" of the primary mesons. For example, a "u$\bar{d}$" primary meson has the flavor of a π^+ or equally well a ρ^+. In this section, we will discuss everything in terms of the pseudoscalars and in the next section include the

possibility of forming vectors or other resonances as well. We assume, as in FF1, that new $q\bar{q}$ pairs are $u\bar{u}$ with probability γ_u, $d\bar{d}$ with equal probability γ_d and $s\bar{s}$ with probability γ_s. From isospin symmetry $\gamma_u = \gamma_d = \gamma$, say, so $\gamma_s = 1 - 2\gamma$. As in FF1, we suppose that strange $s\bar{s}$ pairs are half as likely as unstrange $u\bar{u}$ pairs so that *

$$\gamma = 0.4 \,. \tag{2.24}$$

Let the primary meson states be defined by quark labels "$a\bar{b}$", etc., where a is u, d, or s and likewise for b. A sum on such a label is a sum on u, d, and s. Our assumptions about flavor mean that if the ranks of successive primary mesons are 1, 2, 3, ..., then their flavors must be of the type of a chain $a\bar{b}$ for the first with some $\bar{b}$, then $b\bar{c}$ for the second, $c\bar{d}$ for the third, etc., as shown in fig. 1. The probability of finding them with various momenta is still (2.3) but multiplied by the factor $\gamma_b, \gamma_c, \gamma_d, \ldots$ giving the chance that the correct new pairs $b\bar{b}$, $c\bar{c}$, $d\bar{d}$, ... were indeed formed. It is now easy to modify what we did earlier in subsect. 2.2 for flavor.

For example, for a quark of type q, the mean number of primary meson states of type "$a\bar{b}$" at z is, in analogy to eq. (2.5),

$$P_q^{a\bar{b}}(z) = \delta_{qa}\gamma_b f(1-z) + \int f(\eta) \sum_c \gamma_c P_c^{a\bar{b}}(z/\eta) \,. \tag{2.25}$$

The first term arises because the "$a\bar{b}$" primary meson state might be of first rank (only if a = q, of course, hence the delta function δ_{aq}) with probability $f(1-z)$ times the chance, γ_b, that the first new pair is of the required type b. The second term occurs if the "$a\bar{b}$" primary meson is not of first rank in hierarchy. The first pair might be $c\bar{c}$ (with probability γ_c) and leave a momentum η to the cascade of quark c (with probability $f(\eta)$) in which cascade we find an "$a\bar{b}$" state with probability $P_c^{a\bar{b}}(z/\eta)\, dz/\eta$.

It is seen that the flavor distribution of the 2nd and higher rank primary mesons are independent of what quark started the cascade because we have assumed the new pairs are made with flavors independent of the quark flavor that makes the cascade. Defining a "mean quark" flavor to be $\langle q \rangle$, and equal to u, d, and s with probability γ, γ, and $(1 - 2\gamma)$, respectively, we write

$$P_{\langle q \rangle}^{a\bar{b}}(z) = \sum_c \gamma_c P_c^{a\bar{b}}(z) \,. \tag{2.26}$$

* It is not unreasonable that $s\bar{s}$ pairs are formed less often than $u\bar{u}$ and $d\bar{d}$, for s quarks may have a larger mass than u or d. For example, in a vector force field (e.g. $F = eE$ where E is an electric field and e is the charge on a particle) constant in space and time, the rate of production of pairs of particles of rest mass m and transverse momentum $\boldsymbol{k}_\perp$ ($\boldsymbol{k}_\perp$ is a two-dimensional vector transverse to the direction of the field, the particle has transverse momentum $\boldsymbol{k}_\perp$, the antiparticle $-\boldsymbol{k}_\perp$) is, according to the Dirac equation,

$$(F/2\pi) \exp(-\pi(m^2 + k_\perp^2)/F)\, d^2k_\perp/(2\pi)^2$$

per unit volume per second. Thus it is more difficult to make pairs of mass m by a factor $\exp(-\pi m^2/F)$.

The quantity $P_{\langle q \rangle}$ appears on the right hand side of eq. (2.25) so multiplying by γ_q and summing on q leaves

$$P^{a\bar{b}}_{\langle q \rangle}(z) = \gamma_a \gamma_b f(1-z) + \int f(\eta) P^{a\bar{b}}_{\langle q \rangle}(z/\eta)\, d\eta/\eta \,, \tag{2.27}$$

which, after comparing with (2.5), yields

$$P^{a\bar{b}}_{\langle q \rangle}(z) = \gamma_a \gamma_b F(z) \,. \tag{2.28}$$

Thus if we know the distribution of primary mesons $F(z)$ from quarks disregarding flavor, then those of flavor "$a\bar{b}$" occur in the "mean quark" cascade with probabilities, $\gamma_a \gamma_b$, that the first and the second quark of the pair "$a\bar{b}$" have the appropriate flavors. Only the contribution of the first-rank quark differs from the average. Substituting back into eq. (2.25) and integrating, one finds in general that

$$P^{a\bar{b}}_{q}(z) = \delta_{qa} \gamma_b f(1-z) + \gamma_a \gamma_b \bar{F}(z) \,, \tag{2.29a}$$

where

$$\bar{F}(z) = F(z) - f(1-z) \tag{2.29b}$$

is the probability of finding a primary meson at z of rank higher than one, and $F(z)$ and $f(1-z)$ are the functions given in (2.21) and (2.23).

To be more explicit, the distributions of primary meson states of flavor h from a quark q are given by

$$D^h_q(z) = A^h_q f(1-z) + B^h \bar{F}(z) \,, \tag{2.30}$$

where A^h_q and $B^h = \Sigma_q \gamma_q A^h_q$ have the values given in table 1. For example, the quark content of an eta meson is given by $\eta = S \cos\theta_M + N \sin\theta_M$, where $N = \sqrt{\frac{1}{2}}(u\bar{u} + d\bar{d})$ and $S = s\bar{s}$. Thus, the quantity A^η_u is given by $\frac{1}{2}\gamma \sin^2\theta_M$, where γ is the probability of producing a $\bar{u}$ quark ($\bar{u}u$ pair) to combine with the initial u and $\frac{1}{2}\sin^2\theta_M$ is the chance that this $\bar{u}u$ pair actually forms the desired η.

For now we shall assume all primary mesons are pseudoscalar mesons with no decays. To compare with FF1, we find from table 1 with $\gamma = 0.4$

$$D(z) \equiv D^{\pi^+}_u(z) + D^{\pi^-}_u(z) = 0.32\bar{F}(z) + 0.40 f(1-z) \,, \tag{2.31a}$$

$$K_u(z) \equiv D^{K^+}_u(z) + D^{K^-}_u(z) = 0.16\bar{F}(z) + 0.20 f(1-z) \,, \tag{2.31b}$$

$$K_s(z) \equiv D^{K^+}_s(z) + D^{K^-}_s(z) = 0.16\bar{F}(z) + 0.40 f(1-z) \,; \tag{2.31c}$$

in addition we have

$$D^{\pi^+}_u(z) - D^{\pi^-}_u(z) = 0.4 f(1-z) \,, \tag{2.32a}$$

$$D^{K^+}_u(z) - D^{K^-}_u(z) = 0.2 f(1-z) \,, \tag{2.32b}$$

Table 1
Values of the constants A^i_q, B^i, where q is the quark flavor and i is the primary meson flavor

	$\pi^+(\rho^+)$	$\pi^0(\rho^0)$	$\pi^-(\rho^-)$	$K^+(K^{*+})$	$K^0(K^{*0})$	$K^-(K^{*-})$	$\bar{K}^0(\bar{K}^{*0})$	$\eta(\omega)$	$\eta'(\phi)$
A^i_u	γ	$\frac{1}{2}\gamma$	0	$(1-2\gamma)$	0	0	0	$\frac{1}{2}\gamma \sin^2\theta_M$	$\frac{1}{2}\gamma \cos^2\theta_M$
A^i_d	0	$\frac{1}{2}\gamma$	γ	0	$(1-2\gamma)$	0	0	$\frac{1}{2}\gamma \sin^2\theta_M$	$\frac{1}{2}\gamma \cos^2\theta_M$
A^i_s	0	0	0	0	0	γ	γ	$(1-2\gamma)\cos^2\theta_M$	$(1-2\gamma)\sin^2\theta_M$
B^i	γ^2	γ^2	γ^2	$\gamma(1-2\gamma)$	$\gamma(1-2\gamma)$	$\gamma(1-2\gamma)$	$\gamma(1-2\gamma)$	$\gamma^2 \sin^2\theta_M$ $+(1-2\gamma)^2\cos^2\theta_M$	$\cos^2\theta_M\gamma^2$ $+(1-2\gamma)^2\sin^2\theta_M$

The quantity θ_M is the mixing angle defined by $\eta(\omega) = S\cos\theta_M + N\sin\theta_M$, $\eta'(\phi) = -S\sin\theta_M + N\cos\theta_M$, where $S = s\bar{s}$ and $N = \sqrt{\frac{1}{2}}(u\bar{u} + d\bar{d})$ and where we use $\theta_M = \theta_{ps} = 45°$ and $\theta_M = \theta_v = 90°$ for the pseudoscalar and vector nonets, respectively.

$$D_s^{K^-}(z) - D_s^{K^+}(z) = 0.4\, f(1-z)\,, \tag{2.32c}$$

$$D_u^{K^+}(z) = 0.5\, D_u^{\pi^+}(z)\,, \tag{2.32d}$$

$$D_u^{K^-}(z) = 0.5\, D_u^{\pi^-}(z)\,. \tag{2.32e}$$

These last two equations imply

$$D_u^{K^-}(z)/D_u^{K^+}(z) = D_u^{\pi^-}(z)/D_u^{\pi^+}(z)\,, \tag{2.33}$$

which is what we assumed in eq. (3.7) of FF1. In addition, we have

$$D_u^{\pi^-}(z)/D_u^{\pi^+}(z) = \frac{\gamma^2 \bar{F}(z)}{\gamma f(1-z) + \gamma^2 \bar{F}(z)}\,, \tag{2.34}$$

which approaches zero as z becomes large. This was another of our assumptions in FF1 and here it is a consequence of the property that at $z = 1$, the primary meson must contain the original quark (i.e., $F(z) = f(1-z)$ at $z = 1$ so $\bar{F}(z) \to 0$).

For this case, where all the primary mesons are pseudoscalars with no subsequent decay, the best choice for parameter a in (2.21) and (2.23) is $a = 0.88$. This is determined in fig. 3 by requiring that the model (dashed curve) agree with the lepton data on the charged-particle distribution $D_q^{h^+}(z) + D_q^{h^-}(z)$ and with the earlier FF1 choice (solid curve). The value a is chosen so that $D_q^{h^+}(z = 1) + D_q^{h^-}(z = 1) = 0.6(1 - a)$ agrees with the FF1 curve at $z = 1$.

The fraction of the total momentum carried by each type of primary meson is given by

$$\int z P_q^{a\bar{b}}(z)\, dz = \delta_{qa}\gamma_b \bar{z} + \gamma_a \gamma_b (1 - \bar{z})\,, \tag{2.35}$$

where

$$\bar{z} = \int z f(1-z)\, dz \tag{2.36a}$$

is the mean momentum of the first hierarchy meson and is given by

$$\bar{z} = \tfrac{1}{2} - \tfrac{1}{4}a, \tag{2.36b}$$

for $f(\eta)$ as in (2.21). The momentum carried by the various hadrons with $a = 0.88$ is given in table 2. In FF1 we did not include the η and η' explicitly and, as can be seen from table 2, if we allow the η and η' to decay then the model reproduces the results of FF1 quite closely.

It is of interest to ask how the charges of the primary mesons are distributed along the direction of the initial quark. Suppose we have some quantity such as charge Q, (or third component of isospin I_3, or hypercharge Y) that can be calculated for a primary meson state additively from the quark content of that meson

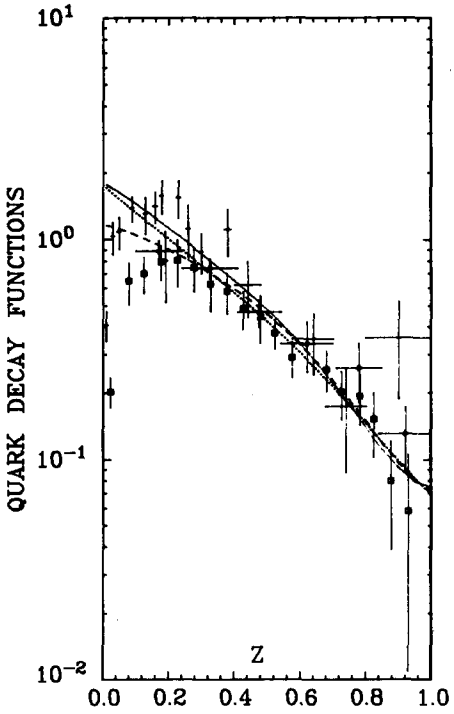

Fig. 3. Comparison of the charged particle distribution $D_u^{h^+}(z) + D_u^{h^-}(z)$ from the quark-jet model with $a = 0.88$, $\alpha_{ps} = 1$, $\alpha_v = 0$ (dashed curve) and with $a = 0.77$, $\alpha_{ps} = \alpha_v = 0.5$ (dotted curve) with the lepton data from fig. 6 of FF1 and with the distribution used in FF1 (solid line). (There is an error in the captions to fig. 6 and fig. 7a in FF1. The ep data from Daken et al. has been averaged over the *two* Q^2 bins $1.0 \leq Q^2 \leq 2.0$ GeV^2 *and* $2.0 \leq Q^2 \leq 3.0$ GeV^2 with $12 < s < 30$ GeV^2.) □ $zN(e^+e^- \to h^\pm)$; ◇ $zN(ep \to h^\pm)$; + $zN(\nu p \to h^\pm)$.

such that each quark flavor, "a", carries e_a and each antiquark $\bar{a}$ contributes $-e_a$. Then if we weigh each primary meson, $a\bar{b}$, by its charge $e_a - e_b$, we obtain the net mean charge distribution of a quark jet. Namely,

$$\langle Q_q(z)\rangle = \sum_{a,b} (e_a - e_b) P_q^{a\bar{b}}(z) = (e_q - e_{\langle q\rangle}) f(1-z)\,, \tag{2.37}$$

from (2.29), where

$$e_{\langle q\rangle} = \sum_a \gamma_a e_a \tag{2.38}$$

is the charge of a "mean" quark. Thus the hadrons in each jet carry a total mean charge, $e_q - e_{\langle q\rangle}$, equal to the charge on the quark producing the jet *plus* a constant error, $-e_{\langle q\rangle}$, proportional to the deviation of the probability of production of new

Table 2
Fraction of the total momentum of a u-, d- and s-quark carried by the primary mesons (before decay, called direct) resulting from our jet model with $a = 0.88$, $\alpha_{ps} = 1.0$, and $\alpha_v = 0.0$. In addition, the results are shown for the total mesons (direct + indirect) after the η and η' are allowed to decay. For comparison, the values from table 2 of FF1 are also given (see also table 6).

		$a = 0.88$, $\alpha_{ps} = 1$ results			FF1 results		
		u	d	s	u	d	s
direct	π^+	0.23	0.12	0.12			
	π^0	0.17	0.17	0.12			
	π^-	0.12	0.23	0.12			
	total π	0.51	0.51	0.35			
	$\eta + \eta'$	0.20	0.20	0.20			
direct + indirect	π^+	0.26	0.15	0.15	0.27	0.15	0.15
	π^0	0.24	0.24	0.18	0.21	0.21	0.15
	π^-	0.15	0.26	0.15	0.15	0.27	0.15
	total π	0.65	0.65	0.48	0.63	0.63	0.45
	K^+	0.11	0.06	0.06	0.13	0.08	0.08
	K^0	0.06	0.11	0.06	0.08	0.13	0.08
	K^-	0.06	0.06	0.17	0.08	0.08	0.19
	$\bar{K}^0$	0.06	0.06	0.17	0.08	0.08	0.19
	total K	0.29	0.29	0.45	0.37	0.37	0.54
	γ	0.06	0.06	0.06			

pairs from the SU(3) value of $\frac{1}{3}$. For the case of electric charge, we have $e_{\langle q \rangle} = \gamma - \frac{1}{3}$ and thus the mean total charge of a quark jet is

$$\langle Q_u \rangle = 1 - \gamma = 0.60 , \tag{2.39}$$

$$\langle Q_d \rangle = -\gamma = -0.40 , \tag{2.40}$$

$$\langle Q_s \rangle = -\gamma = -0.40 , \tag{2.41}$$

which is in close agreement with the empirically fitted values of 0.59, –0.40, and –0.39, respectively, found in FF1. The mean total I_3 is just the I_3 of the quark, independent of γ since I_3 of the mean quark is zero (u and d coming with equal weight). Hypercharge, Y is $2(Q - I_3)$, so its mean for u- and d-quark jets is 0.2 and for s-quark jets is –0.8.

The charge on the jet of a "mean" quark is $\Sigma_q \gamma_q (e_q - e_{\langle q \rangle}) = 0$ so that the second and higher hierarchy primary mesons carry no charge on the average. Thus, were it not for complications from secondary disintegrations, which we discuss later, the experimental determination of the net mean charge, $\Sigma_h e_h D_q^h(z)$, where e_h is the charge of the hadron h, would give a direct measure of the distribution of the first-rank primary meson, $f(1 - z)$.

At first sight one might wonder why the total average charge of the hadrons is not that of the original quark, because after all, the new quark pairs $q\bar{q}$ are each neutral. However, as pointed out by Rosner and Farrar [11] and by Cahn and Colglasier [12], for a jet starting from a quark, each new pair has its antiquark going into a hadron of one lower rank in the hierarchy than does its quark. The new antiquark has, on the average, the higher momentum. Thus, when we consider all the hadrons higher than some very small momentum z_0 (small enough to ensure that the mean number of positive and negative hadrons in dz are practically the same), we are counting more antiquarks than quarks. This makes no difference for isospin, since we have $\bar{u}$ and $\bar{d}$ antiquarks equally likely, but the average electric charge of antiquarks is not zero but is given by $e_{\langle\bar{q}\rangle} = (-\frac{2}{3} + \frac{1}{3})\gamma + \frac{1}{3}(1 - 2\gamma)$. The $\bar{s}$ quarks are not in their full number, $\frac{1}{3}$, needed to cancel the average $\bar{u} + \bar{d}$ charge. Since, in counting charge, only mesons (we leave out the complication and slight numerical modification due to baryon production) are counted, the total number of quarks and antiquarks counted must be exactly the same. Therefore, we must succeed in counting an excess of exactly one antiquark over quarks from the new pairs, to compensate the extra quark from which the jet started. Thus, the charges of all hadrons above z_0 exceed that of the original quark e_q by the charge of one mean antiquark $e_{\langle\bar{q}\rangle} = -e_{\langle q\rangle}$ (about $-\frac{1}{15}$ charge units). For this reason, the net charge of a "mean" quark jet is zero. This last result can also be seen in the following way. In a "mean" quark jet, all the mesons are formed out of pairs of "mean" quarks and "mean" antiquarks. Any tendency of the antiquark of one new pair to combine with a quark of lower rank to make a meson has no effect, for that lower-rank quark is also a "mean" quark with the same probability of flavors as the antiquark. In the general case, charge imbalance can be seen, in the mean, only in the hadron containing the original quark as indicated by (2.37).

We now turn to the problem of generalizing the double-decay function in (2.12) to include the effects of correlations in flavor. We define

$$P_q^{a\bar{b},c\bar{d}}(z_1, z_2)\, dz_1\, dz_2 = \text{probability of finding a primary meson of flavor "}a\bar{b}\text{" at } z_1 \textit{ and} \text{ one of flavor "}c\bar{d}\text{" at } z_2 \text{ in a jet originated by a quark of flavor q when the primary meson at } z_2 \text{ has a larger rank in hierarchy than the one at } z_1. \tag{2.42}$$

This probability is the sum of the following four pieces.

(i) The probability that the primary meson at z_1 is of rank 1 and the primary meson at z_2 is of rank 2; given by

$$\delta_{qa}\gamma_b\delta_{bc}\gamma_d f(1 - z_1)\, dz_1 f(1 - z_2/(1 - z_1))\, \frac{dz_2}{1 - z_1}\,. \tag{2.43a}$$

For this term q = a and b is arbitrary with probability γ_b, but then c = b and d comes with probability γ_d. The probability that z_1 is rank-1 is $f(1 - z_1)\, dz_1$, and

then since $1 - z_1$ momentum is left, the probability that z_2 is second-rank (i.e., rank-1 in the remaining hierarchy) is $f(1 - z_2/(1 - z_1))\,dz_2/(1 - z_1)$.

(ii) The probability that z_1 is of rank one, but z_2 is of rank higher than 2:

$$\delta_{qa}\gamma_b\gamma_c\gamma_d f(1 - z_1)\,dz_1 \bar{F}(z_2/(1 - z_1))\frac{dz_2}{1 - z_1}\,. \tag{2.43b}$$

For this case, the chance to get $c\bar{d}$ is now independent of q, a, and b and is $\gamma_c\gamma_d$.

(iii) The probability that the primary meson at z_1 is not first in rank but higher, but the primary meson at z_2 is directly of next rank to the one at z_1:

$$\gamma_a\gamma_b\delta_{bc}\gamma_d \int_{z_1+z_2}^{1} g(\eta)\,d\eta f(1 - z_1/\eta)\frac{dz_1}{\eta} f(1 - z_2/(\eta - z_1))\frac{dz_2}{\eta - z_1}\,, \tag{2.43c}$$

where the early primary mesons leave momentum η (with probability $g(\eta)\,d\eta$) and the next two primary mesons come as rank one and two. Here the flavor of q has no affect, a and b come with probability $\gamma_a\gamma_b$, but c must equal b. We must, of course, integrate over all remaining momenta η.

(iv) Neither the primary meson at z_1 or z_2 is first in rank, nor are they adjacent:

$$\gamma_a\gamma_b\gamma_c\gamma_d \int_{z_1+z_2}^{1} g(\eta)\,d\eta f(1 - z_1/\eta)\frac{dz_1}{\eta}\bar{F}(z_2/(\eta - z_1))\frac{dz_2}{\eta - z_1}\,. \tag{2.43d}$$

The complete double-fragmentation function for producing two hadrons of flavor $h_1 = a\bar{b}$ and $h_2 = cd$ is given by symmetrizing (2.43a–d) with respect to z_1 and z_2. Namely,

$$\tilde{P}_q^{a\bar{b},\,c\bar{d}}(z_1, z_2) = P_q^{a\bar{b},\,c\bar{d}}(z_1, z_2) + P_q^{c\bar{d},\,a\bar{b}}(z_2, z_1)\,. \tag{2.44}$$

2.6. *The production of resonances*

Finally, we must decide in what nonet a primary meson is formed. We suppose that the pair of quarks $q\bar{q}$ is in the low pseudoscalar 0^- configuration with the probability α_{ps}, that it is a vector meson 1^- with probability α_v, a tensor meson 2^+ with probability α_t, etc. Then these objects are allowed to disintegrate as we know they should from the particle tables.

We suppose that the choices of the probabilities α are dynamic and do not depend on the flavor. Although attempts have been made to determine from hadron experiments the production rate of, say, ρ^0 compared to π^0 at larger $p_\perp$, the experiments are difficult to interpret. Indications are that ρ^0 is roughly as likely as π^0 at high $p_\perp$ (see references in table 16) and that higher resonances are less likely [13]. For definiteness for the present, we shall choose

$$\alpha_{ps} = \alpha_v = 0.5\,, \tag{2.45}$$

with no higher resonances * ($\alpha_t = 0$, etc.), which yields $D_u^{\rho^0}(z)/D_u^{\pi^0}(z) \to 1$ as $z \to 1$. Future experiments may, however, indicate a better choice.

2.7. The Monte Carlo method

2.7.1. Recursive scheme

The method of Monte Carlo generation of a complete quark cascade is clear. Suppose one starts with a quark of flavor q and momentum W_0. Then

(i) One generates a value of $\eta_1 = 1 - z_1$ at random with probability given by $f(\eta)$ as in eq. (2.21).

(ii) One generates a quark pair $u\bar{u}$, $d\bar{d}$, or $s\bar{s}$ with probability γ, γ, and $(1-2\gamma)$ (i.e., 0.4, 0.4, and 0.2), respectively. The first primary meson state is then of type $q\bar{u}$, $q\bar{d}$, or $q\bar{s}$ depending on the pair chosen.

(iii) One decides on the spin-parity of the primary meson, according to (2.45), (i.e., pseudoscalar or vector with equal probabilities.

The first primary meson is now of momentum $(1-\eta_1)W_0$ and of type $q\bar{u}$, $q\bar{d}$ or $q\bar{s}$ depending on the choice made in (ii) and of spin depending on the choice made in (iii). This leaves, for the next step, a quark of type q_2 = u, d, or s (depending on the first quark pair chosen) with momentum $W_1 = \eta_1 W_0$. The cycle beginning with (i)–(iii) is then repeated for this quark q_2 with momentum W_1. Another η value is found and a new quark pair produced. This procedure is then repeated over and over until a desired point, to be discussed later (sect. 3 below), is reached.

Finally, we add transverse momentum according to subsect. 2.7.2 and then let the vector mesons decay, each with its known characteristic kinematics and branching ratios, as given in the particle tables. In addition, we allow the η and η' mesons to decay.

As discussed earlier, in choosing the spin-parity of the primary mesons (iii), we assume that α_{ps} and α_v are independent of flavor. For example, a $u\bar{u}$ primary meson state is a π^0 with probability $\frac{1}{2}\alpha_{ps}$, an η with probability $\frac{1}{2}\alpha_{ps}\sin^2\theta_{ps}$, an η' with probability $\frac{1}{2}\alpha_{ps}\cos^2\theta_{ps}$, a ρ^0 with probability $\frac{1}{2}\alpha_v$, a ω^0 with probability $\frac{1}{2}\alpha_v\sin^2\theta_v$ and a ϕ^0 with probability $\frac{1}{2}\alpha_v\cos^2\theta_v$ in agreement with table 1. The pseudoscalar and vector mixing angles θ_{ps} and θ_v are chosen to be 45° and 90°, respectively.

2.7.2. Including transverse momentum

The hadrons arising from the cascade or fragmentation of a quark do not travel in precisely the same direction as the initiating quark (i.e., z direction). We expect that the transverse momentum of these hadrons remains limited as the quark's momentum becomes large; however, we really have no knowledge as to the precise manner in which the various hadrons share the transverse momentum. One can imagine several ways to distribute transverse momentum among the primary mesons

* The theoretical idea that the quark spins combine randomly would recommend, rather, that $\alpha_v = 3\alpha_{ps}$.

in our jets. We will choose a particular way, not because we are sure it is nature's way, but for definiteness. Very few of the results in this paper depend on this particular choice.

We will incorporate transverse momentum into our model by assuming that the quark-antiquark pairs $q_i\bar{q}_i$ which are produced to discharge the color field conserve transverse momentum in a pairwise fashion and have no net transverse momentum. The quark q_i in the ith pair is assigned a transverse momentum $\boldsymbol{q}_{\perp_i}$ and the antiquark the balancing momentum $-\boldsymbol{q}_{\perp_i}$. The $\boldsymbol{q}_{\perp_i}$ are distributed according to the Gaussian distribution

$$\exp(-q_{\perp_i}^2/2\sigma_q^2)\, d^2q_\perp . \tag{2.46}$$

Except for the first-rank primary meson, all primary mesons are given a transverse momentum that is the vector sum of the transverse momenta of the two quarks which form it. The first-rank primary meson is assigned a transverse momentum given by

$$\boldsymbol{k}_\perp(1) = \boldsymbol{q}_{\perp_1} - \boldsymbol{q}_{\perp_0} , \tag{2.47a}$$

the second-rank primary meson

$$\boldsymbol{k}_\perp(2) = \boldsymbol{q}_{\perp_2} - \boldsymbol{q}_{\perp_1} , \tag{2.47b}$$

and the rth-rank primary meson

$$\boldsymbol{k}_\perp(r) = \boldsymbol{q}_{\perp_r} - \boldsymbol{q}_{\perp_{r-1}} : \tag{2.47c}$$

The initial $\boldsymbol{q}_{\perp_0}$ is also generated according to (2.46). This is to insure that the first primary meson has the same mean square transverse momentum as the others.

The net result is to produce a cascade of primary mesons all of which have the same distribution of transverse momentum at fixed z, a Gaussian with a mean $\langle k_\perp^2\rangle = 2\sigma^2$ and

$$\langle k_\perp\rangle_{\text{primary mesons}} = \sqrt{\tfrac{1}{2}\pi}\sigma , \tag{2.48a}$$

with

$$\sigma = \sqrt{2}\,\sigma_q , \tag{2.48b}$$

since two quarks contribute to each primary meson. This method introduces a correlation between primary mesons of adjacent rank, so that they tend to go oppositely, the mean of $(\boldsymbol{k}_{\perp_1} \cdot \boldsymbol{k}_{\perp_2})$ is $-\sigma^2$. There is no correlation between primary mesons whose rank is not adjacent. The physical ideas are reasonable enough, but the particular choice of $\langle(\boldsymbol{k}_{\perp_1} \cdot \boldsymbol{k}_{\perp_2})\rangle = -\sigma^2$ is a pure guess. It is made so that the total perpendicular momentum of the jet $\boldsymbol{k}_{\perp_{\text{jet}}} = \boldsymbol{k}_{\perp_1} + \boldsymbol{k}_{\perp_2} + \ldots + \boldsymbol{k}_{\perp_N}$ has a mean square which does not rise with N.

In general, we could also contemplate another parameter giving the center of mass of the new pairs a Gaussian distribution. This has the affect of decreasing the negative correlation coefficient $\langle \boldsymbol{k}_{\perp_1} \cdot \boldsymbol{k}_{\perp_2}\rangle / \sqrt{\langle k_{\perp_1}^2\rangle \langle k_{\perp_2}^2\rangle}$ between adjacent-rank

primary mesons from the value $-\frac{1}{2}$ to any value minus or plus up to $+\frac{1}{2}$ depending on parameters. In this case, extra rules would have to be added to keep the sum $k_{\perp_{\text{jet}}}$ within bounds, and rather than risk complications, we do not do this.

Our main aim for adding transverse momentum is to study the differences between the true rapidity Y and $Y_z = -\ln z$ and to investigate the effect of resonance decays on the distributions of transverse momentum. In addition, it will be interesting to see if there is any experimental indication that primary mesons adjacent in rank have negative transverse momentum correlations. Unfortunately, as we will discover in sect. 5, although the correlation is close in hierarchy, it is spread over a wide range in rapidity due to the mixing of rank in hierarchy and order in rapidity, and is further obscured by correlations between mesons coming from the decay of the same primary.

The value of the deviation σ in (2.48a) is chosen so that the finally observed charged pions (those produced directly as primary mesons *plus* those resulting from secondary decays of primary vector mesons) have a mean $k_\perp$ of

$$\langle k_\perp \rangle_{\pi^\pm} = 323 \text{ MeV} . \tag{2.49a}$$

This requires a choice of

$$\sigma = 350 \text{ MeV} \tag{2.49b}$$

and results in

$$\langle k_\perp \rangle_{\text{primary mesons}} = 439 \text{ MeV} . \tag{2.49c}$$

The difference between the mean transverse momentum of the primary mesons and the resulting observed pions is due to resonance decay and the significance of this will be discussed in detail in sect. 5.

2.7.3. Finite-momentum jets

When discussing the Monte Carlo method of generating jets, (i)–(iii) in subsect. 2.7.1, we avoided mentioning at what point one terminates the iterations. The procedure, as outlined, would produce a jet of infinite momentum, an infinite number of particles, and an infinitely long rapidity plateau. For a jet of very large momentum P in the z direction, there is no problem. One merely continues to produce particles until all the available momentum P is used up. For large P, for any z not too small, $p_z = zP$ is large enough that questions such as the difference between energy $E = \sqrt{p_z^2 + m^2 + P_\perp^2}$ and p_z are not important. But what shall we do for real jets of finite momentum P? Even if P is a few GeV so that we can take it equal to the energy, for smaller z (say, $z < 0.2$), one has ambiguities. In the plateau, we know how to resolve such ambiguities. The $dz/z = dp_z/p_z$ behavior in the plateau comes from relativistic phase-space factors multiplying matrix elements which are slowly varying so that the dz/z should be replaced by dp_z/E. But this is exactly $d(E + p_z)/(E + p_z)$. We shall thus resolve all ambiguities by interpreting all variables ξ, W, etc., to refer not to momentum but rather to the quantity $E + p_z = p_z + \sqrt{p_z^2 + m^2 + P_\perp^2}$. The

variable z in $F(z)$ and $f(1-z)$ in eqs. (2.23) and (2.21) with $\eta = 1-z$ and similarly in all our equations refers to

$$z = (E + p_z)/(E_0 + p_{z_0}) , \tag{2.50}$$

where $E_0 + p_{z_0}$ is for the initial quark. Since the initial quark will always have fairly large momenta, we can replace $E_0 + p_{z_0}$ by $2P_0$, where P_0 is the initial quark momentum. Eq. (2.23) should be reasonable as long as p_z is not too large negative.

For energies large enough that a plateau region is developed, experience with inelastic hadron collisions shows us that scaling and limiting fragmentation hold approximately. This implies that a plot of hadron distributions *versus* rapidity

$$Y = \tfrac{1}{2} \ln((E + p_z)/(E - p_z)) = \ln(E + p_z) - \ln m_\perp , \tag{2.51a}$$

where

$$m_\perp^2 = m^2 + P_\perp^2 , \tag{2.51b}$$

has a simple property. The distribution of particles moving to the right in, say, the c.m.s., are the same for different energy collisions if only the origin of the rapidity Y axis is shifted by Y_0, the rapidity of the original right-moving beam. This is equivalent to the principle that the distribution of particles moving near one end and into the plateau, but not near the other end of the distribution, for one energy can be obtained from that of another energy simply by a Lorentz transformation in the $\hat{z}$ direction. This is because such a Lorentz transformation by a velocity v simply multiplies all $E + p_z$ by a common factor, $\sqrt{(1-v)/(1+v)}$, and does not affect rapidity differences or $E + p_z$ ratios. We shall assume that the same is true of our quark jets.

Jets of finite momentum are produced by first generating "master" jets of very large momentum P_0. Each primary meson has a mass m_i, a perpendicular momentum $\boldsymbol{P}_{\perp_i}$ generated according to subsect. 2.7.2, and an $E_i + p_{z_i}$ determined from

$$E_i + P_{z_i} = z_i(E_0 + P_0) , \tag{2.52}$$

where z_i is generated by the procedures of subsect. 2.7.1. The primary mesons are then allowed to decay according to the rates in the particle tables and jets of finite quark momentum P_q are produced by computing a new or scaled $(E + p_z)_{new}$ by

$$(E + p_z)_{new} = (E + p_z)_{old}(E_q + P_q)/(E_0 + P_0) \tag{2.53a}$$

and keeping all final mesons such that

$$(p_z)_{new} \geqslant 0 . \tag{2.53b}$$

Resonance decays are relatively simple to handle under this scheme. The primary mesons determined according to (2.52) are allowed to decay and the Lorentz transformations of z_i are easy as already mentioned. The sum of the z's of the decay products are equal to the z of the parent. However, occasionally parents with $p_{z_i} \leqslant 0$ will produce a decay product with $p_z \geqslant 0$. We are defining our jets to have only forward-moving particles and thus include such decay products with $p_z \geqslant 0$

Table 3
Mean multiplicity of all particles $\langle N \rangle$, charged particles $\langle N_{ch} \rangle$, positive particles $\langle N_+ \rangle$ and negative particles $\langle N_- \rangle$ for u-quark jets of various energies P_q resulting from the jet model with $a = 0.77$ and $\alpha_{ps} = \alpha_v = 0.5$. Also shown in the "correlation moment" $f_2 = \langle N(N-1) \rangle - \langle N \rangle^2$.

P_q (GeV)	3.5	10	50	500
$\langle N_{tot} \rangle$	4.6	8.2	14.1	22.6
f_2^{tot}	−1.3	2.2	12.9	33.4
$\langle N_{ch} \rangle$	2.7	4.8	8.2	13.0
f_2^{ch}	−0.8	0.2	3.3	9.5
$\langle N_+ \rangle$	1.6	2.7	4.4	6.8
f_2^+	−0.8	−1.1	−1.2	−0.9
$\langle N_- \rangle$	1.1	2.1	3.8	6.2
f_2^-	−0.4	−0.6	−0.6	−0.3

even though the parent was moving backward. Likewise, we exclude backward-moving secondaries even if the parent was moving forward.

Real quark jets cannot have both the energy and momentum of a free quark of definite mass *. However, it must be remembered that all quark jets occur in pairs. In e^+e^- collisions, two jets result from the $q\bar{q}$ pair produced. In νp reactions, one jet results from the quark "knocked out" of the proton by the neutrino and the other from the "hole" that was left behind. In hadron-hadron collisions at high $p_\perp$, according to the model in FF1, we may think of a quark as being knocked out of the proton by another quark and "generating" a color field as the quark pulls away from the "hole" it left behind. This results in a four-jet structure as discussed in ref. [5] (hereafter called FFF). Energy and momentum are conserved in the two-jet system *not* for the single jet. Hence, any quantity like energy or $k_\perp$ that is not conserved in the single jet is balanced by its oppositely moving partner.

Our quark jets do not precisely conserve energy or momentum. For example, a $P_q = 10$ GeV quark jet produced in the above manner has mean values $\langle E_{tot} \rangle = 9.8$ GeV and $\langle p_{z_{tot}} \rangle = 8.6$ GeV, where E_{tot} and $p_{z_{tot}}$ are the total energy and p_z of all the hadrons in the jet. The mean value of $E_{tot} + p_{z_{tot}}$ does approach $2P_q$ at high momentum. Rather than compensate for the fact that our cut-off procedure yields $E_{tot} + p_{z_{tot}}$ less than $2p_z$ at finite P_q, we can interpret our jets as having an *energy* equal to P_q since this comes out closely the same without any adjustment. For all P_q, the mean value of $E_{tot} - p_{z_{tot}}$ is about 1.2 GeV, and $\langle k_{\perp_{jet}} \rangle$ is about 610 MeV, where $k_{\perp_{jet}}$ is the total perpendicular momentum of all the hadrons in the jet.

Finally, in table 3, we show the particle multiplicities resulting using the above

* If one selects $E + p_z$ of all hadrons in the jet to equal the $E + p_z$ of a large momentum initial quark, then $E - p_z$ is equal to the mean density of particles in the plateau times the $m_\perp$ of the particles. See the discussion on p. 246 of ref. [14].

cut-off prescription. The table gives the mean multiplicity of all particles, charged particles, positive particles, and negative particles for a u-quark with energy $P_q = 3.5$, 10.0, 50.0, and 500.0 GeV, arrived at with $a = 0.77$ and $\alpha_{ps} = \alpha_v = 0.5$.

2.8. *The analytic approximation*

Although the Monte Carlo method is straightforward, some jet observables require the generation of a large number of typical jets in order to get sufficient statistical accuracy. In addition, it is very handy to have analytic formulas for easy analysis and understanding and so the reader can, without writing a Monte Carlo program, reproduce most of our results. For these reasons, we present approximate analytic solutions for those observables where analytic methods are not too difficult. Details of individual resonance decay are too tedious to handle exactly analytically. What we have done is to assume all products of vector meson decay are distributed as they would be in a two-body isotropic decay of massless products; that is spread uniformly in z from 0 to the z of the parent. Thus for all vector decays, we assume the daughter-parent relationship

$$\hat{G}(z) = 2\int_z^1 G(z/y)\,dy/y\,, \tag{2.54}$$

where $\hat{G}(z)$ is the distribution in z of a daughter of parents distributed in $G(z)$. The integral of (2.54) is easy for $G(z) = F(z)$ or $G(z) = f(1-z)$, since if $G(z) = z^n$ then $\hat{G}(z) = 2(1-z^n)/n$ for $n \neq 0$ and $-2\ln z$ for $n = 0$.

The total distribution of hadrons is

$$F_{\text{total}}(z) = \alpha_{ps}F(z) + \alpha_v\hat{F}(z)\,, \tag{2.55}$$

and the distribution of the first-rank meson is

$$f_{\text{total}}(1-z) = \alpha_{ps}f(1-z) + \alpha_v\hat{f}(1-z)\,, \tag{2.56}$$

where we assign all the decay products the rank in hierarchy of their parent primary meson and where α_{ps} and α_v, given by (2.45), are the relative strengths of the pseudoscalar and vector meson component. The values of $\alpha_{ps}zF(z)$, $\alpha_{ps}f(1-z)$, $\alpha_v z\hat{F}(z)$, and $\alpha_v\hat{f}(1-z)$ are given in fig. 2b with $a = 0.77$. As can be seen in fig. 3, the choice $a = 0.77$, $\alpha_{ps} = \alpha_v = 0.5$ produces a good fit to the lepton data on the charged particle z distribution and compares well with the FF1 result.

The distribution of hadrons of flavor h from a quark q is given by

$$D_q^h(z) = \alpha_{ps}[A_q^h f(1-z) + B^h\bar{F}(z)] + \alpha_v[\hat{A}_q^h\hat{f}(1-z) + \hat{B}^h\hat{\bar{F}}(z)]\,, \tag{2.57}$$

where $\bar{F}(z)$ is the probability that the meson at z has any rank greater than one and is defined by (2.29b). (Similarly, $\hat{\bar{F}}(z) = \hat{F}(z) - \hat{f}(1-z)$.) The constants $\hat{A}_q^h$ and $\hat{B}^h$

are given by

$$\hat{A}_q^h = \sum_{i=1}^{9} \beta_{i\to h} A_q^i \,, \tag{2.58a}$$

$$\hat{B}^h = \sum_{i=1}^{9} \beta_{i\to h} B^i \,, \tag{2.58b}$$

where the sum is over all nine vector mesons and $\beta_{i\to h}$ is the probability that one finds a daughter of type h as a decay product of a parent of type i. The constants A_q^h and B^h are as in (2.30) and are given in table 1 (for vector production one uses $\theta_M = \theta_v$ and for pseudoscalar production one uses $\theta_M = \theta_{ps}$). The ρ and K^* resonances decay 100% of the time to $\pi\pi$ and $K\pi$, respectively, and the $\beta_{i\to h}$ are easily calculable from isospin symmetry. The values used for $\beta_{i\to h}$ for ω and ϕ are given in table 4, where we approximate three-body decays by the two-body decay formula (2.54) but with $\beta_{i\to h}$ adjusted to give the correct frequency into the various mesons. For example, we take $\omega \to \pi^+\pi^-\pi^0$ and $\omega \to \pi^0\gamma$ with a 90% and 10% rate, respectively, so that $\beta_{\omega\to\pi^\pm} = \frac{1}{3}(0.90)$ and $\beta_{\omega\to\pi^0} = \frac{1}{3}(0.90) + \frac{1}{2}(0.10)$.

In addition, to agree better with the Monte Carlo results, we have also allowed the η and η' to decay. These decays are handled in the same manner (2.54) as the vector meson ω decay but with the $\beta_{i\to h}$ given in table 4.

Fig. 4 shows a comparison of the analytic approximation and the more precise Monte Carlo method. Agreement is good except for the pions resulting from the ω^0 decay (similarly for three body η and η' decay modes) which have been approximated by the two-body decay formula. The approximation for $K^{*0} \to K^+$ does not agree as well as $\rho^0 \to \pi^+$ due to the heavier mass of the K.

The inclusion of resonance decays into the analytic formula for the double-decay distribution $P_q^{a\bar{b},c\bar{d}}(z_1, z_2)$ given by (2.42) and (2.43) is straightforward. One

Table 4
Probability $\beta_{i\to h}$ to find a daughter meson of type h among all the decay products of a parent meson of type i

Parent / Daughter	η	η'	ω	ϕ
π^+	0.09	0.27	0.30	0.06
π^0	0.40	0.24	0.35	0.06
π^-	0.09	0.27	0.30	0.06
K^+	0	0	0	0.24
K^0	0	0	0	0.17
K^-	0	0	0	0.24
$\bar{K}^0$	0	0	0	0.17

For $i = \rho$ and K^*, $\beta_{i\to h}$ is given by isospin symmetry assuming $\rho \to \pi\pi$ and $K^* \to K\pi$ 100% of the time.

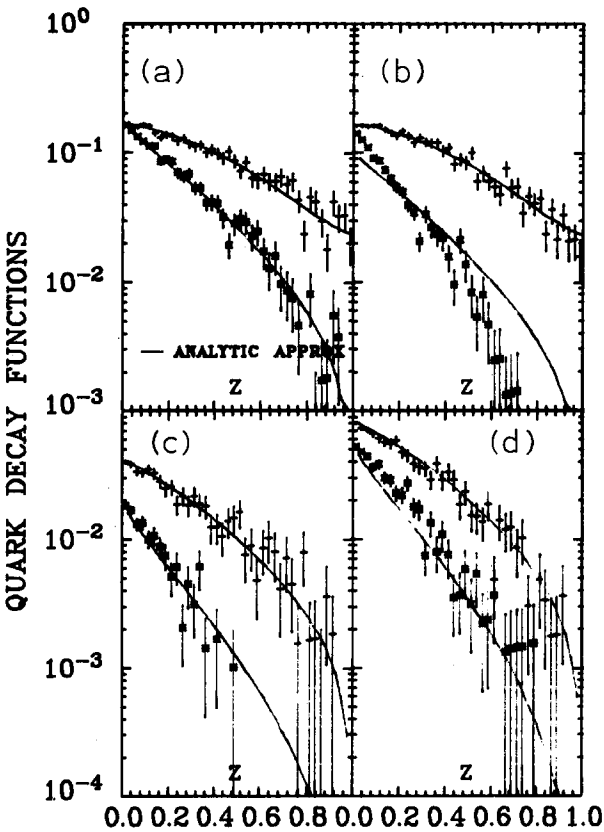

Fig. 4. Comparison of the Monte Carlo results ($a = 0.77$, $\alpha_{ps} = \alpha_v = 0.5$) for some of the quark-decay functions, $D_q^h(z)$, with the analytic approximation (solid curve). The number of ρ^0, ω^0, ϕ, and K^{*0} from a u-quark are shown together with the number of π^+ that have decayed from ρ^0 and ω^0 and the number K^+ from ϕ and K^{*0}. (a) + $zD(u \to \rho^0)$; x $zD(u \to \rho^0 \to \pi^+)$; (b) + $zD(u \to \omega^0)$; x $zD(u \to \omega^0 \to \pi^+)$; (c) + $zD(u \to \phi)$; x $zD(u \to \phi \to K^+)$; (d) + $zD(u \to K^{*0})$; x $zD(u \to K^{+0} \to K^+)$.

merely replaces the $F(z)$ and $f(1-z)$ functions in (2.43) by the $F_{total}(z)$ and $f_{total}(1-z)$ functions in (2.55) and (2.56). From this $D_q^{h_1 h_2}(z_1, z_2)$ is computed in a manner analogous to (2.57). In addition, however, one must add the contribution from the case where both the mesons at z_1 and z_2 came from the decay of the same resonance (type h_v) given by

$$B_{h_v \to h_1, h_2} D_q^{h_v}(z_1 + z_2)/(z_1 + z_2)\,, \tag{2.59}$$

where $D_q^{h_v}(z)$ is the single-particle distribution of the parent h_v and $B_{h_v \to h_1, h_2}$ in its branching ratio into $h_1 = a\bar{b}$ and $h_2 = c\bar{d}$.

Table 5
Description of the parameters used in the model of quark jets and an explanation of how they are determined

Parameter	Description	Determination
a	Parameter used to describe the function $f(\eta) = 1 - a + 3a\eta^2$, which is the probability that the first-rank primary meson leaves a fraction of momentum η to the remaining cascade.	Require that resulting charged distribution $D_q^{h^+}(z)$ fit the data shown in fig. 3.
γ	The probability of producing a $u\bar{u}$, $d\bar{d}$, and $s\bar{s}$ pair is given by γ, γ, and $(1-2\gamma)$, respectively.	Use the fact that at large $p_\perp$ in pp collisions $K^+/\pi^+ = \frac{1}{2}$. Requiring $D_u^{K^+}(z)/D_u^{\pi^+}(z) = \frac{1}{2}$ as $z \to 1$ then implies $\gamma \approx 0.4$.
α_{ps}, α_v	Relative probability of producing a pseudoscalar meson or a vector meson ($\alpha_{ps} + \alpha_v = 1$).	Experiments indicate that $\rho^0/\pi^0 \simeq 1$ at large $p_\perp$ in pp collisions so we choose $\alpha_{ps} = \alpha_v = 0.5$.
σ	Determines the $\langle k_\perp \rangle$ of the produced primary mesons.	Require $\langle k_\perp \rangle_\pi$ near 330. Means $\langle k_\perp \rangle_{primary} = 439 = \sqrt{\frac{1}{2}\pi}\,\sigma$.
θ_{ps}, θ_v	Pseudoscalar and vector nonet mixing angles where $\eta(\omega) = S\cos\theta + N\sin\theta$, $\eta'(\phi) = -S\sin\theta + N\cos\theta$, with $S = s\bar{s}$, $N = \sqrt{\frac{1}{2}}(u\bar{u} + d\bar{d})$.	Use $\theta_{ps} = 45°$ and $\theta_v = 90°$ as simple numbers close to experiment.
$\beta_{i\to h}$	Probability to find a daughter meson of type h among all the decay products of a parent vector meson of type i.	Use branching ratios in particle tables.

Our model of quark jets is thus completely determined by the function $f(\eta)$, which we have parametrized by a parabola with one parameter, a, and the three additional parameters; the degree that SU(3) is broken in the formation of new $q\bar{q}$ pairs (γ in (2.24)), the spin-parity nature of the primary mesons (α_{ps}, α_v in (2.45)) and the mean transverse momentum of the primary mesons (σ in (2.48a)). From this, all the properties of quark jets follow. The parameters of the model together with a review of how they were determined is given in table 5. We now proceed to examine the results of the model in detail.

3. Properties of the "end" of the quark jet

3.1. *Single-particle distribution* $D_q^h(z)$

Figs. 5, 6, and 7 show the single-particle quark-decay functions, $D_q^h(z)$, resulting from our new jet model with $a = 0.77$ and $\alpha_{ps} = \alpha_v = 0.5$ together with the analytic

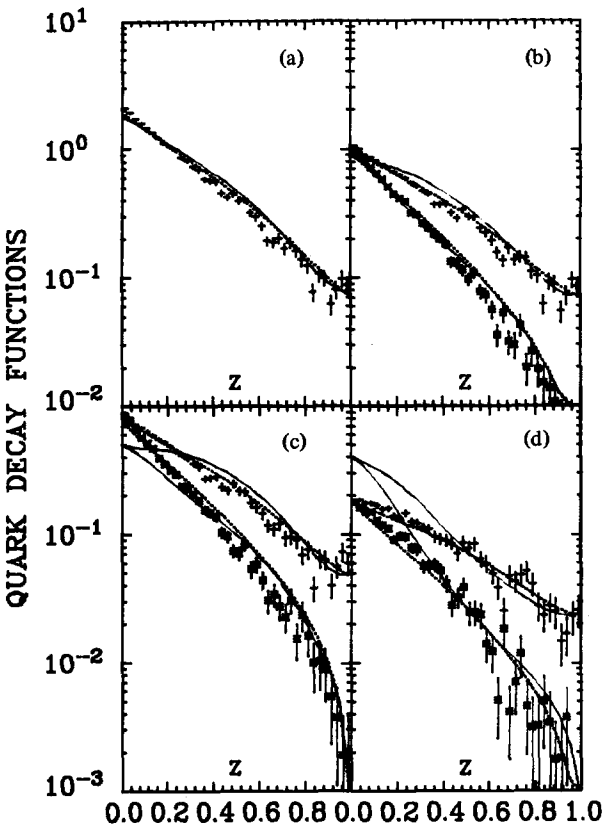

Fig. 5. The quark-decay functions (a) $zD(u \to h^+ + h^-, z)$; (b) $zD(u \to h^{\pm}, z)$, + $zD(u \to h^+)$, x $zD(u - h^-)$; (c) $zD(u \to \pi^{\pm}, z)$, + $zD(u \to \pi^+)$, x $zD(u \to \pi^-)$; and (d) $zD(u \to K^{\pm}, z)$, + $zD(u \to K^+)$, x $zD(u \to K^-)$, resulting from the quark-jet model with $a = 0.77$ and $\alpha_{ps} = \alpha_v = 0.5$ (points). Also shown is the analytic approximation (dotted curve) and the results obtained in FF1 (solid curves).

approximation (dotted curve). For comparison, the results arrived at in FF1 are also displayed (solid curves). The differences between the analytic calculations and the Monte Carlo results are because in the analytic approximation, we have considered all decays as massless two-body decays. For instance, as seen in fig. 4 the $\omega \to 3\pi$ decay is not treated correctly in the analytic approximation. Nevertheless, the two methods agree quite closely.

The decay functions in figs. 5, 6, and 7 agree well for the most part with the results from FF1. There are, however, the following notable differences.

(i) The new decay functions have

$$D_u^{K^{\pm}}(z)/D_u^{\pi^{\pm}}(z) \underset{z \to 0}{\to} 0.2\,, \tag{3.1}$$

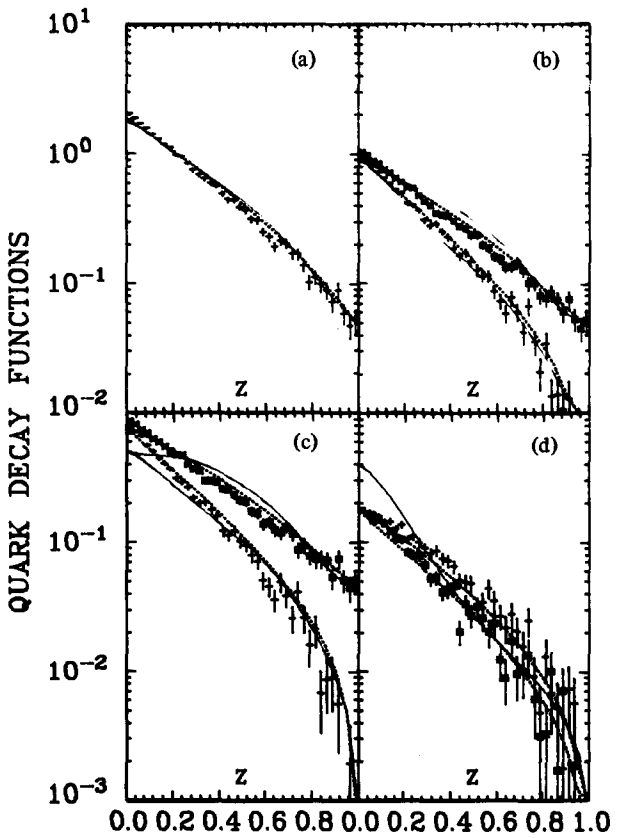

Fig. 6. Same as fig. 5 but for a d-quark.

whereas the FF1 results yield a value of 0.8. Both have

$$D_u^{K^\pm}(z)/D_u^{\pi^\pm}(z) \underset{z\to 1}{\to} 0.5, \tag{3.2}$$

by construction, since $\gamma = 0.4$. The difference at small z is due to the many K^* resonances that decay into kaons *and* pions. The new results are probably more reasonable than the FF1 values.

(ii) The new approach yields

$$D_d^{K^+}(z) > D_d^{K^-}(z), \tag{3.3}$$

whereas in FF1 we assumed equality for simplicity. However, as discussed in FF1, (3.3) is expected.

Table 6 gives the total fraction of momentum carried by the direct (primary)

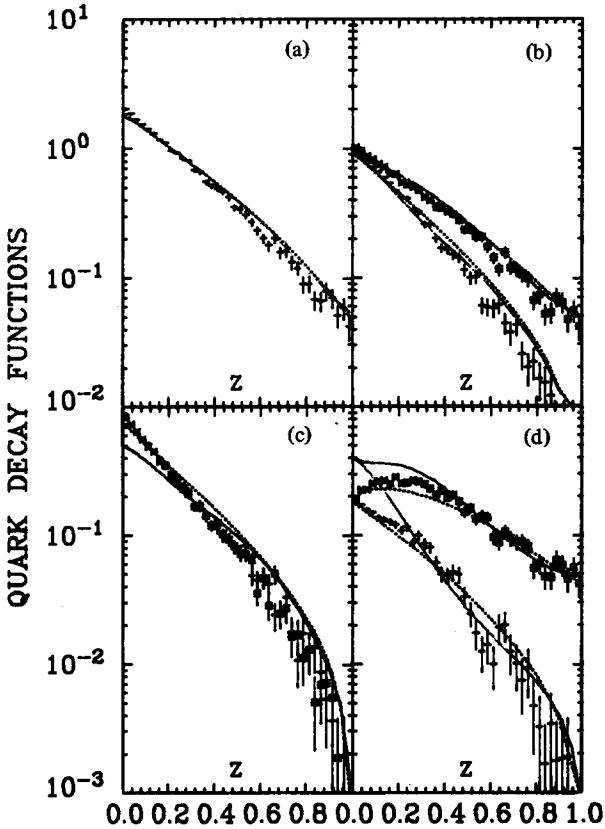

Fig. 7. Same as fig. 5 but for an s-quark.

mesons and by the final hadrons (direct + decay) for a u-, d-, and s-quark. These results can be compared to the FF1 values shown in table 2.

In spite of the differences at small z between our new results and the FF1 results, they are not very different for large z ($z \geq 0.6$). Since the large-$p_\perp$ single-particle predictions made in FF1 and most of the two-particle correlation results obtained in FFF (ref. [5]) are only sensitive to the large-z region of the quark decay functions, most of the predictions made in FF1 and FFF remain unchanged. Changes and improvements of the results of FF1 and FFF will be discussed in sect. 6.

3.2. Approach to the rapidity plateau

Figs. 8, 9, and 10 show the number of hadrons, charged hadrons, positive hadrons and negative hadrons per 0.1 unit of Y_z for a u-, d- and s-quark, respectively. We

Table 6
Fraction of total momentum carried by the direct-primary (before decay) mesons and the direct-plus-indirect (from a decay) mesons resulting from a u-, d- and s-quark in our jet model with $a = 0.77$ and $\alpha_{ps} = \alpha_v = 0.5$

	Particle	u	d	s
Direct	$\pi^+ = \rho^+$	0.12	0.06	0.06
	$\pi^0 = \rho^0$	0.09	0.09	0.06
	$\pi^- = \rho^-$	0.06	0.12	0.06
	$K^+ = K^{*+}$	0.06	0.03	0.03
	$K^0 = K^{*0}$	0.03	0.06	0.03
	$K^- = K^{*-}$	0.03	0.03	0.09
	$\bar{K}^0 = \bar{K}^{*0}$	0.03	0.03	0.09
	η	0.05	0.05	0.05
	η'	0.05	0.05	0.05
	ω	0.09	0.09	0.06
	ϕ	0.01	0.01	0.04
total = direct + indirect	π^+	0.29	0.19	0.19
	π^0	0.26	0.26	0.20
	π^-	0.19	0.29	0.19
	K^+	0.08	0.06	0.06
	K^0	0.06	0.08	0.06
	K^-	0.04	0.04	0.13
	$\bar{K}^0$	0.04	0.04	0.13
	γ	0.04	0.04	0.04
total	π	0.74	0.74	0.58
total	K	0.22	0.22	0.38

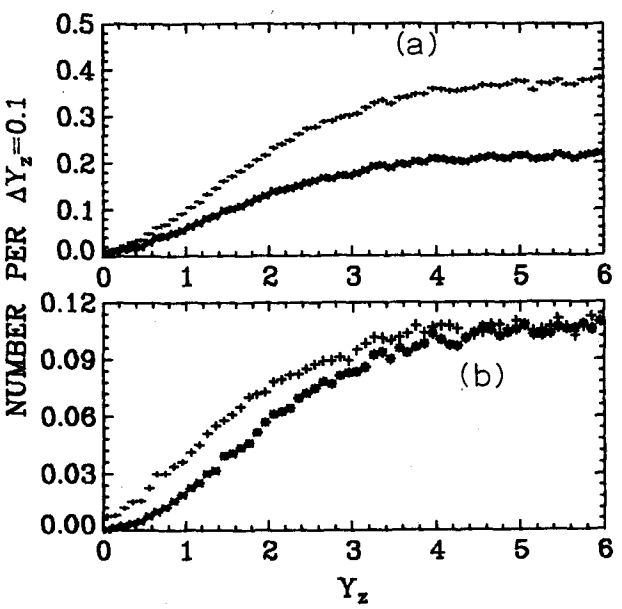

Fig. 8. The number of particles, charged particles, positive particles and negative particles per $\Delta Y_z = 0.1$ resulting from a u-quark jet with $a = 0.77$ and $\alpha_{ps} = \alpha_v = 0.5$, where $Y_z = -\ln z$. (a) + all particles; x charged particles; (b) + positive particles, x negative particles.

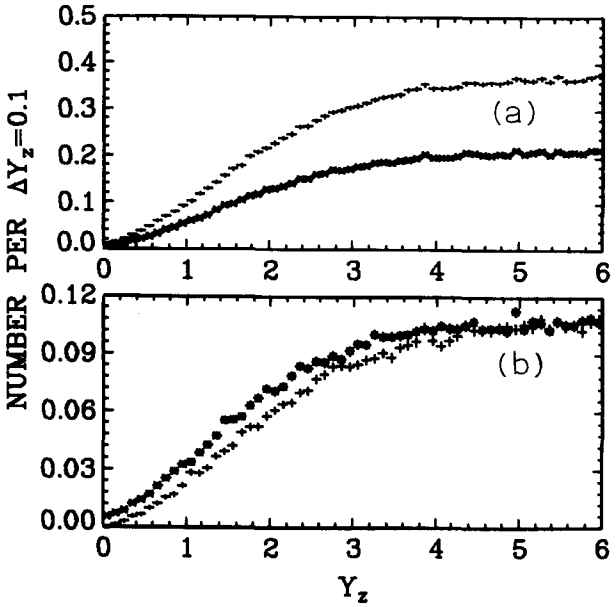

Fig. 9. Same as fig. 8 but for a d-quark jet.

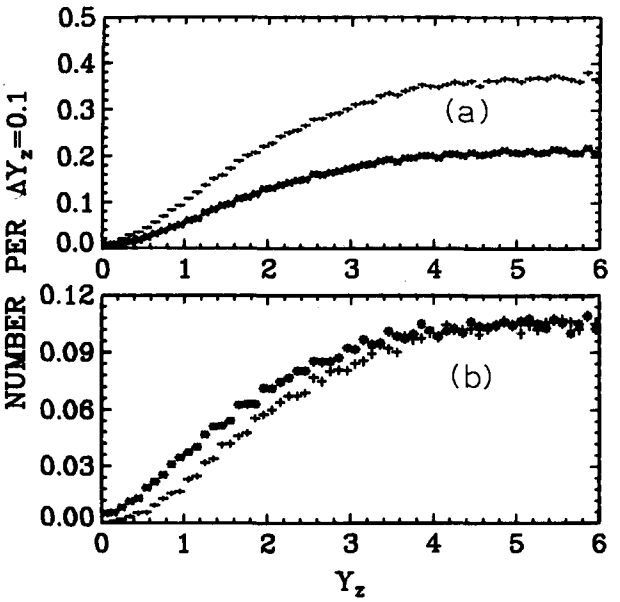

Fig. 10. Same as fig. 8 but for an s-quark jet.

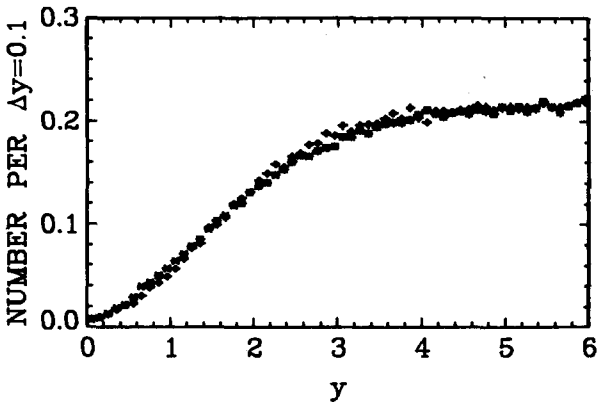

Fig. 11. Comparison of the number of charged particles per $\Delta Y_z = 0.1$ *versus* Y_z with the number of charged particles per $\Delta Y = 0.1$ *versus* $Y_{\text{end}} - Y$ for a u-quark jet, where $Y_z = -\ln z$ and Y is the true rapidity (2.51) and Y_{end} is given by (3.6b) with $m_{\perp_0} \approx 380$ MeV. $a = 0.77$, $\alpha_{\text{ps}} = \alpha_{\text{v}} = 0.5$, $\diamond\, y = Y_{\text{end}} - Y$, $\times\, y = Y_z$.

have defined the "z rapidity", Y_z, by

$$Y_z = -\ln z = -\ln((E + p_z)/2P_{\text{q}}) \,. \tag{3.4}$$

This is a convenient variable for us since it does not depend on the generated value of the perpendicular mass, $m_\perp$, in equation (2.51b). The usual rapidity, Y, is given by (2.51a) and hence

$$Y = -Y_z + \ln(2P_{\text{q}}/m_\perp) \,, \tag{3.5}$$

so that particles at the same Y_z may be found spread a bit in Y because of differences of mass and transverse momenta. It is usual to measure Y from some Y_{end} at the high-momentum end of the jet. For this one might expect to take $\ln(2P_{\text{q}}/m_{\text{q}})$, where m_{q} is the mass of the original quark, but this has no clear meaning. Alternatively, data could be plotted using

$$Y_{\text{max}} = \ln(2P_{\text{q}}/m_\pi) \tag{3.6a}$$

for Y_{end} since this is the maximum rapidity a pion of the jet could have. These differences are, of course, only shifts of scale of Y for convenience in plotting. In fig. 11, we compare the $Y_{\text{end}} - Y$ and Y_z distributions, where we have chosen

$$Y_{\text{end}} = Y_{\text{max}} - \ln(m_{\perp_0}/m_\pi) \,, \tag{3.6b}$$

with $m_{\perp_0}$ an arbitrary number chosen in an attempt to make the two distributions agree. The distributions are nearly identical with $m_{\perp_0} = 380$ MeV, the $Y_{\text{end}} - Y$ distribution being slightly steeper. (This value is close to the mean $m_\perp$.)

The model yields about 2.2 charged particles per unit rapidity in the plateau with equal numbers of positive and negative particles. (Some multiplicities are given in

table 3.) Towards the "end" of the quark jet ($Y_z \lesssim 3$), on the other hand, the number of positive and negative hadrons is not the same and one can hope to discriminate among the quark flavors by observations in this region of Y_z.

3.3. Distribution of charge

Any single-quark jet has an integral number of hadrons and an integral charge. The average total charge of a u-, d- and s-quark jet of infinite momentum is nearly the charge of the quark (for $\gamma = 0.4$ we have 0.6, −0.4, and −0.4 as shown in (2.39)). Table 7 shows the number of times various total jet charges Q occur for 10 000 jets with energy $P_q = 10$ GeV. Jets initiated by u-quarks are more likely to have positive total charge than those initiated by d-quarks. For example, at $P_q = 10$ GeV, $Q = +2$ jets occur $\simeq 4$ times more often for u-jets than for d-jets and $Q = +4$ jets occur

Table 7
Number of times various total quark-jet charge Q occurred for 10 000 quark jets with energy $P_q = 10$ GeV

Charge Q	u	d	s
−4	7	39	42
−3	42	231	227
−2	307	1094	1115
−1	1291	2972	3009
0	3118	3675	3661
1	3460	1576	1483
2	1398	340	390
3	299	62	60
4	64	6	7
$\langle Q \rangle$ [a]	0.54	−0.36	−0.36

Same as above but observe only those hadrons with $z > 0.1$

Charge Q	u	d	s
−4	2	0	6
−3	20	88	74
−2	258	710	781
−1	1442	2969	3172
0	3560	4123	4091
1	3639	1742	1606
2	967	342	255
3	106	23	15
4	6	3	0
$\langle Q \rangle$	0.39	−0.21	−0.28

[a] For infinite momentum quark jets, the mean charge, $\langle Q \rangle$, is 0.60, −0.40, −0.40 for a u-, d- and s-jet, respectively.

about 10 times more frequently. The average total charge, $\langle Q \rangle$, for a P_q = 10 GeV u- and d-jet is 0.54 and −0.36, respectively. Because of the finite total momentum available (P_q = 10 GeV) summing only $z > 0$ does not yet yield the full total mean charge 0.6 and −0.4 expected. There is some overlap of charge into negative z. An interesting point is that the mean total jet charge $\langle Q \rangle$ is *not* precisely the same for each fixed multiplicity. As table 8a shows, the odd charged multiplicity jets (N_{ch} = 1, 3, etc.) have a mean charge $\langle Q \rangle$ that is somewhat larger than the jets of even charge multiplicity (N_{ch} = 2, 4, etc.). For an extreme example, for u-quark jets having only one charged particle (N_{ch} = 1), that particle is positive about 13 times more often than it is negative ($\langle Q \rangle$ = 0.86).

Unfortunately, total jet charge is often a difficult quantity to measure experimen-

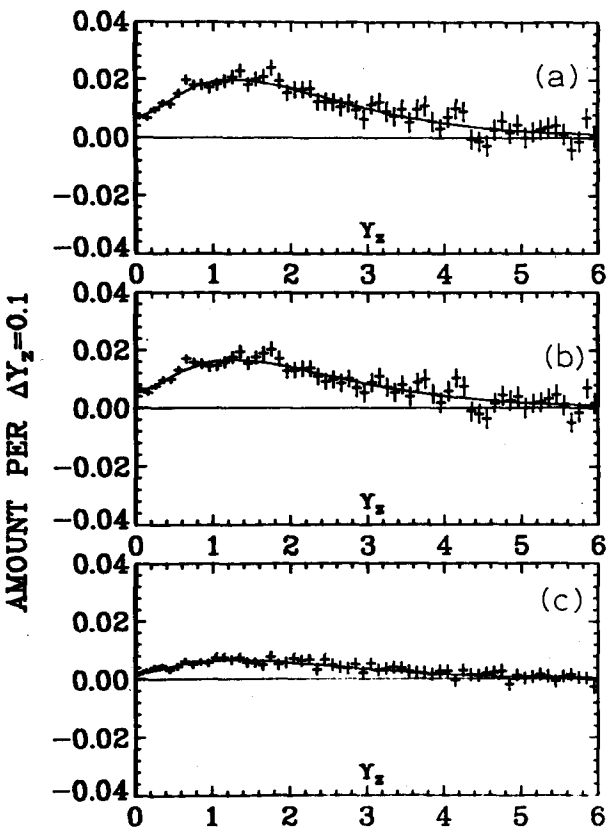

Fig. 12. Distribution of (a) charge Q, total Q = 0.6, (b) third component of isospin I_3, total I_3 = 0.5, and (c) strangeness S, total S = 0.2, along the Y_z ($Y_z = -\ln z$) axis for a u-quark jet. Also shown are the analytic results (solid curves). a = 0.77, $\alpha_{ps} = \alpha_v$ = 0.5.

Table 8a
Number of times various total quark-jet charge Q occurred for 10 000 jets with momentum P_q = 10 GeV, where N_{ch} is the charged multiplicity

		u	d	s
all jets	$Q > 0$	5232	1984	1941
	$Q < 0$	1650	4341	4398
	$Q = 0$	3118	3675	3661
	$\langle Q \rangle$ [a]	0.54	−0.36	−0.36
$N_{ch} = 1$ jets	$Q > 0$	420	102	81
	$Q < 0$	31	287	341
	$\langle Q \rangle$	0.86	−0.48	−0.62
$N_{ch} = 2$ jets	$Q > 0$	175	25	37
	$Q < 0$	13	118	147
	$Q = 0$	591	799	839
	$\langle Q \rangle$	0.42	−0.20	−0.22
$N_{ch} = 3$ jets	$Q > 0$	1029	423	427
	$Q < 0$	266	883	937
	$\langle Q \rangle$	0.64	−0.38	−0.41
N_{ch} = even jets ($N_{ch} \neq 0$)	$Q > 0$	1462	346	397
	$Q < 0$	314	1133	1157
	$Q = 0$	3052	3535	3512
	$\langle Q \rangle$	0.50	−0.33	−0.31
N_{ch} = odd jets	$Q > 0$	3770	1638	1543
	$Q < 0$	1336	3208	3241
	$\langle Q \rangle$	0.58	−0.40	−0.43

[a] For infinite-momentum jets $\langle Q \rangle$ = 0.60, −0.40 and −0.40 for a u-, d- and s-quark, respectively.

tally. One can never be sure that all the jet particles have been included and that one has not included extra background particles. A more tractable quantity experimentally is the total charge of all those hadrons in a jet whose z value exceeds some threshold. As shown in tables 7 and 8b, charges defined for P_q = 10 GeV and $z \geq 0.1$ have the same characteristics as the complete jet but the magnitudes are smaller. The average total charges ($z \geq 0.1$) are 0.39 and −0.21 for a u- and d-jet, respectively.

Figs. 12, 13, and 14 show the distribution of charge Q, third component of isospin I_3, and strangeness S (of course, $S = 2(Q - I_3)$) along the Y_z axis for a u-, d- and s-quark, respectively. As discussed in subsect. 2.5 and given by (2.37), these quantities are related to the distribution of the first-rank primary meson, $f(1-z)$, and the integrated values are given by (2.39), (2.40), and (2.41) (with $S = Y$ since we have no baryons among the resulting hadrons). Also shown in these figures is the analytic approximation. As can be seen, the charge, isospin, and strangeness are distributed

Table 8b
Same as table 8a except only hadrons with $z \geq 0.1$ are observed

		u	d	s
all jets	$Q > 0$	4718	2110	1876
	$Q < 0$	1722	3767	4033
	$Q = 0$	3560	4123	4091
	$\langle Q \rangle$	0.39	−0.21	−0.28
$N_{ch} = 1$ jets	$Q > 0$	2624	1205	1090
	$Q < 0$	936	2120	2272
	$\langle Q \rangle$	0.47	−0.28	−0.35
$N_{ch} = 2$ jets	$Q > 0$	871	309	240
	$Q < 0$	229	651	713
	$Q = 0$	2383	2557	2402
	$\langle Q \rangle$	0.37	−0.19	−0.28
$N_{ch} = 3$ jets	$Q > 0$	1101	551	522
	$Q < 0$	512	918	949
	$\langle Q \rangle$	0.47	−0.33	−0.37
N_{ch} = even jets ($N_{ch} \neq 0$)	$Q > 0$	973	345	255
	$Q < 0$	260	710	787
	$Q = 0$	2607	2792	2643
	$\langle Q \rangle$	0.37	−0.19	−0.29
N_{ch} = odd jets	$Q > 0$	3745	1765	1621
	$Q < 0$	1462	3057	3246
	$\langle Q \rangle$	0.47	−0.29	−0.36

over a considerable range in Y_z. The quark quantum numbers are spread over almost 4 units of Y_z, which will make it difficult to determine them experimentally.

One of the most important experimental questions about high-$p_\perp$ hadron collisions is whether the jets really come from quark cascades as we have supposed in FF1 and FFF, or possibly from other types of objects such as gluons or di-quarks. We have calculated the flavor of the quarks to be expected under various circumstances (see fig. 25 of FFF). When the characteristics of the quark jets of definite flavor in lepton experiments are known, the details can be checked against the jets observed in hadron experiments. But what should we measure to most readily identify the flavor of a quark jet: the total charge, the charge of the fastest hadron, of the fastest two? We have used our model for a "standard" jet as a kind of laboratory of typical jets to test various ideas. The following sections on the flavor properties of the jets, therefore, contain very detailed information from these studies on various quantities which have been selected because they are easy to measure experimentally or because they are expected to differ as much as possible for u- and d-flavor jets.

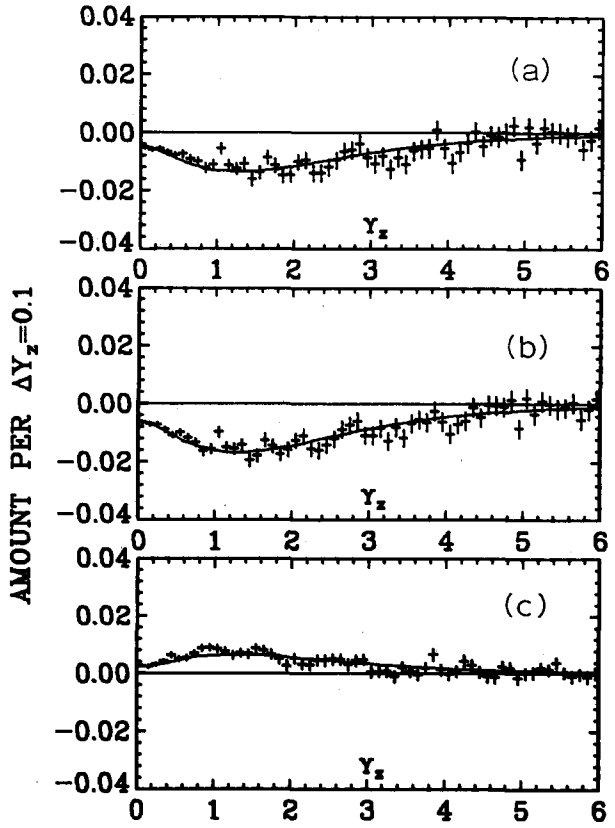

Fig. 13. Same as fig. 12 but for a d-quark jet. (a) Total $Q = -0.4$, (b) total $I_3 = -0.5$, (c) total $S = 0.2$.

3.4. Fastest-particle analysis

It is interesting to ask about the fraction of momentum, z, carried by the fastest hadron (largest z) when a quark fragments into hadrons in an unbiased fashion. Figs. 15 and 16 show the z distributions of various hadrons fragmenting from a u-quark of energy 10 GeV resulting from the model where, by first and second, we mean fastest (largest z) and second-fastest (next-largest z). These figures and table 9 show that for a u-quark jet, the fastest hadron carries on the average only 39% of the quark momentum and the fastest charged hadron only 30%. Fig. 17 and table 10 show that for a u-quark, the fastest charged hadron carries 54% of the total charged momentum with the second fastest charged particle taking about 21%. (All charged particles carry on the average about 57% of the u-quark momentum.) The fastest two

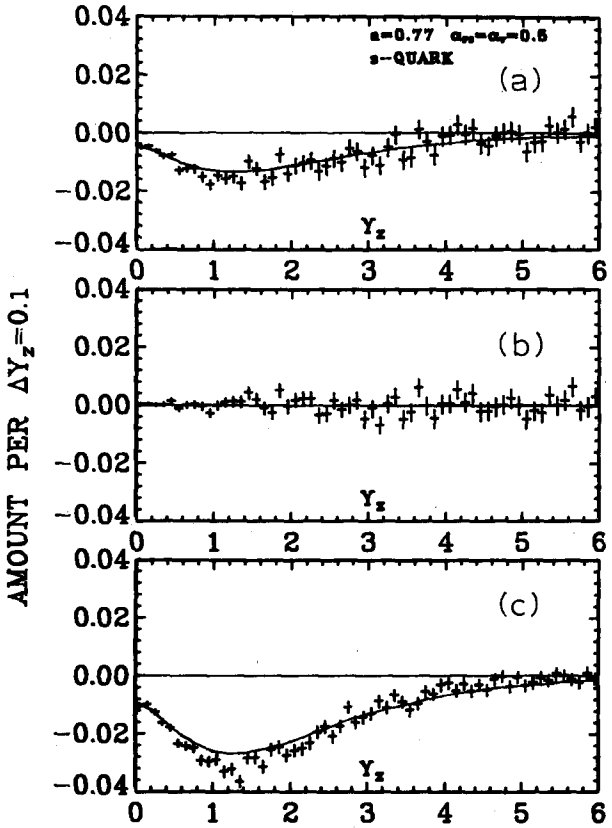

Fig. 14. Same as fig. 12 but for an s-quark jet. (a) Total $Q = -0.4$, (b) total $I_3 = 0.0$, (c) total $S = -0.8$.

Table 9
Mean values of z for hadrons fragmenting from a u-, d- and s-quark of energy $P_q = 10$ GeV

	u	d	s
fastest hadron	0.39	0.39	0.38
2nd-fastest hadron	0.18	0.18	0.19
3rd-fastest hadron	0.11	0.11	0.11
fastest charged	0.30	0.28	0.27
2nd-fastest charged	0.12	0.12	0.12
3rd-fastest charged	0.06	0.06	0.06
all charged	0.57	0.54	0.52
fastest positive	0.25	0.17	0.15
2nd-fastest positive	0.07	0.04	0.04
3rd-fastest positive	0.02	0.01	0.01
fastest negative	0.15	0.22	0.22
2nd-fastest negative	0.04	0.06	0.06
3rd-fastest negative	0.01	0.02	0.02

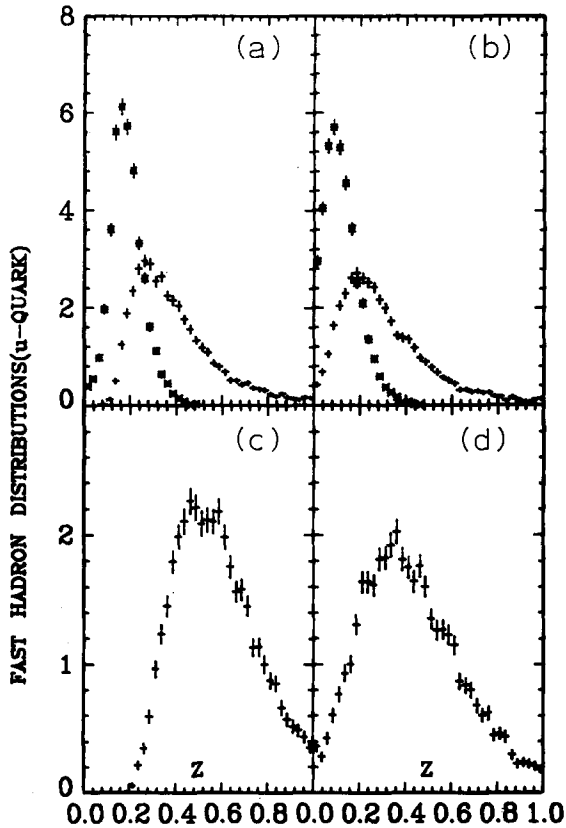

Fig. 15. The predicted z distributions of various hadrons in a u-quark jet with P_q = 10 GeV, where first and second refer to the *fastest* (largest-z) and second *fastest* (next largest-z), *not* to rank in hierarchy. a = 0.77, $\alpha_{ps} = \alpha_v$ = 0.5. (a) + First particle ($\langle z \rangle$ = 0.39), × second particle ($\langle z \rangle$ = 0.18); (b) + first charged ($\langle z \rangle$ = 0.30), × second charged ($\langle z \rangle$ = 0.12), (c) first two particles ($\langle z \rangle$ = 0.57), (d) first two charged ($\langle z \rangle$ = 0.42).

Table 10
Mean values of z_R for hadrons fragmenting from a u-, d- and s-quark of energy P_q = 10 GeV, where $z_R = z/z_{ch}$ and z_{ch} is the sum of the z of all charged hadrons

	u	d	s
Fraction of jets with at least one charged particle	0.993	0.986	0.985
fastest charged	0.54	0.53	0.53
2nd-fastest charged	0.21	0.22	0.22
Fraction of jets with at least one positive particle	0.988	0.943	0.932
fastest positive	0.45	0.31	0.30
2nd-fastest positive	0.12	0.08	0.08
Fraction of jets with at least one negative particle	0.929	0.973	0.972
fastest negative	0.27	0.41	0.42
2nd-fastest negative	0.07	0.11	0.11

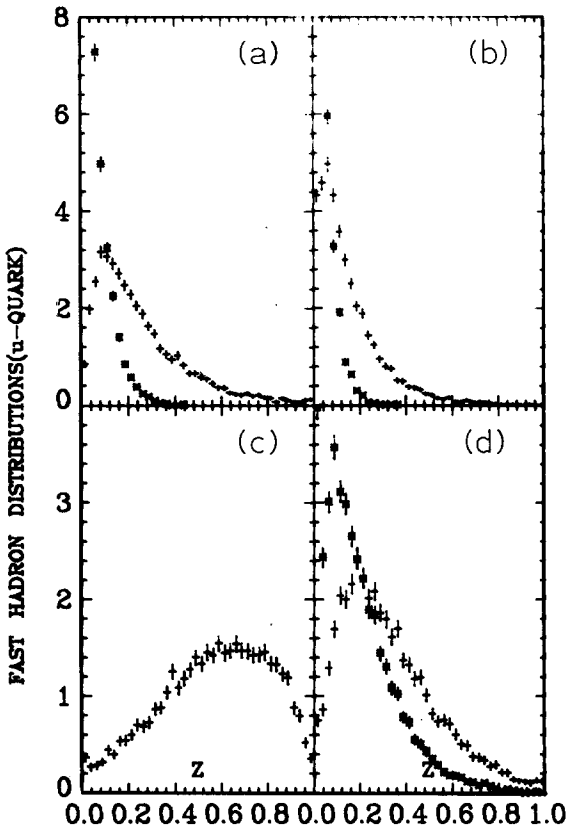

Fig. 16. Same as fig. 15, continued. (a) + First positive ($\langle z \rangle = 0.25$), × second positive ($\langle z \rangle = 0.07$); (b) + First negative ($\langle z \rangle = 0.15$), × second negative ($\langle z \rangle = 0.04$), (c) all charged ($\langle z \rangle = 0.57$), (d) + First two positive ($\langle z \rangle = 0.32$), × first two negative ($\langle z \rangle = 0.19$).

charged hadrons in a u-quark jet carry about 75% of the total charged momentum. Roughly, the fastest charged hadron takes, on the average, half the charged momentum; the second fastest charged hadron takes half the remaining charged momentum, etc. This feature of the model is in agreement with experimental observations of jets produced in νp interactions [15] as seen in fig. 19.

We might have expected, from the point of view from which we began, that the primary meson containing the original quark would be likely to have a large fraction of that quark's momentum. Yet the function $f(1-z)$ in eq. (2.21) shows this primary meson to be more likely to have less than half of the initial quark's momentum. In fact, from (2.36) the average is less than a third of the jet momentum (for $a = 0.77$). Because of this, there is a considerable difference between rank in hierarchy and order

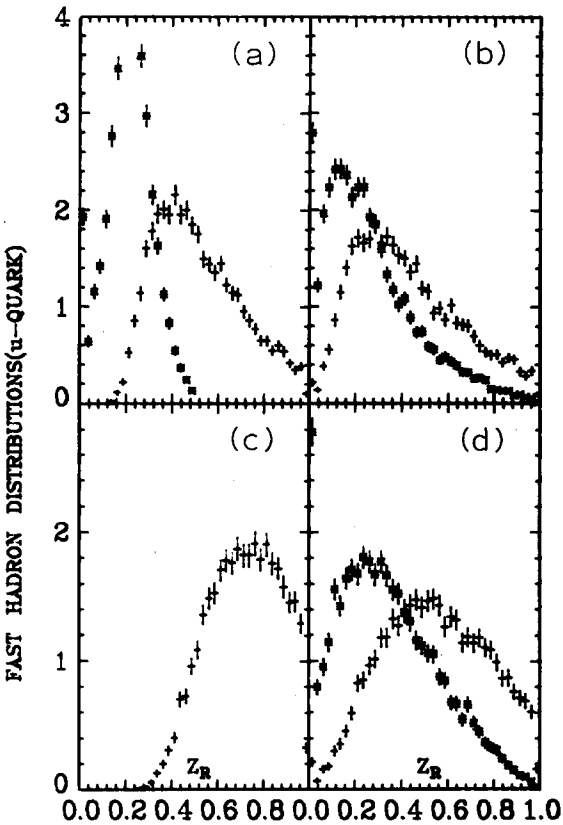

Fig. 17. The predicted z_R distributions of various hadrons in a u-quark jet with P_q = 10 GeV, where z_R is the relative fraction of charged momentum defined by $z_R = z/z_{ch}$ where z_{ch} is the sum of the z's of all charged particles in the jet. As in figs. 15 and 16, first and second refer to order in z *not* to rank in hierarchy. a = 0.77, $\alpha_{ps} = \alpha_v$ = 0.5. (a) + first charged ($\langle z_R \rangle$ = 0.54), × second charged ($\langle z_R \rangle$ = 0.21), (b) first positive ($\langle z_R \rangle$ = 0.45), × first negative ($\langle z_R \rangle$ = 0.27), (c) first two charged ($\langle z_R \rangle$ = 0.75), (d) + first two positive ($\langle z_R \rangle$ = 0.57), × first two negative ($\langle z_R \rangle$ = 0.34).

Table 11
Number of times the fastest (largest-z) hadron occurred with rank r (r = 1, ..., 5) for 10 000 u-quark jets

Rank r	Unbiased	$z \geq 0.5$	$z \geq 0.75$
1	4267	1345	340
2	2566	564	97
3	1506	197	23
4	795	56	3
5	436	17	0
Mean rank	2.3	1.7	1.4

All the decay products of a particular primary meson are assigned the rank of that meson.

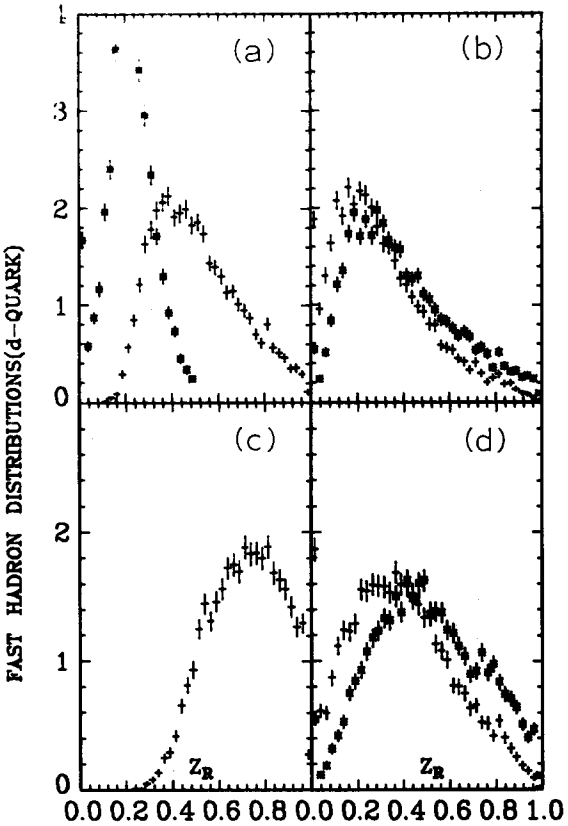

Fig. 18. Same as fig. 17 but for a d-quark jet. (a) + first charged ($\langle z_R \rangle = 0.53$), × second charged ($\langle z_R \rangle = 0.22$), (b) + first positive ($\langle z_R \rangle = 0.31$), × first negative ($\langle z_R \rangle = 0.41$), (c) first two charged ($\langle z_R \rangle = 0.75$), (d) + first two positive ($\langle z_R \rangle = 0.39$), × first two negative ($\langle z_R \rangle = 0.52$).

in rapidity (or z). It is relatively easy for the first-rank primary meson to leave the remaining cascade with a large momentum and thus to end up with a momentum less than some subsequent (higher-rank) meson. Table 11 shows that the fastest hadron from an unbiased u-quark jet is the first-rank meson only 43% of the time. However, as one selects on events where the z of the fastest hadron is large, it becomes more likely that it is of rank-one in hierarchy. For $z \geqslant 0.75$, this probability increases to 73% becoming 100% at $z = 1$.

An interesting property of a jet, that has not yet been tested experimentally, is how the fraction of momentum carried by the fastest hadron in a jet depends on the charge of that hadron. In our model, for a u-quark, the first-rank primary meson can be positive or neutral, *not* negative. A negative hadron can arise only further down the hierarchy chain (rank greater than one) *or* from the decay of a

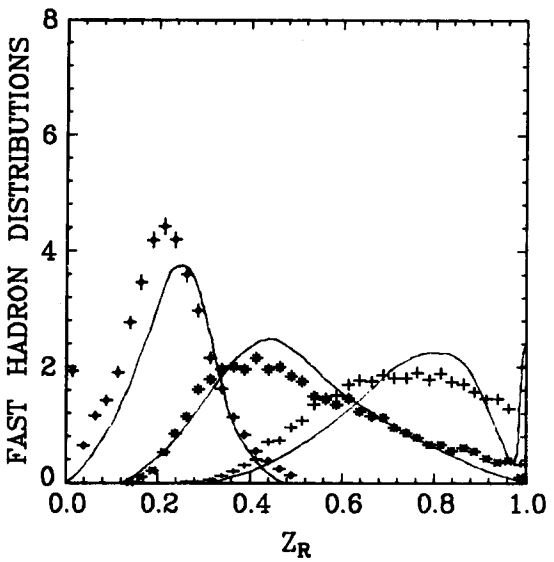

Fig. 19. Comparison of the predicted distributions of z_R for the fastest, second-fastest and fastest two charged hadrons in a u-quark jet (points) with data from $\nu p \to \mu^- +$ jet + X (ref. [15], solid curve), where z_R is the relative fraction of charged momentum as in fig. 17. (Note that in this figure, the theory are the points with errors and the data are represented by the solid curves.) $a = 0.77$, $\alpha_{ps} = \alpha_v = 0.5$, $P_q = 10$ GeV. x first charged, ◇ second charged, + first two charged, —— neutrino data.

rank-one neutral resonance. Because of this, the fastest positive hadron in a u-quark jet carries, on the average, a larger portion of the total momentum (45%) than does the fastest negative hadron (27%). Results of this type are tabulated in table 10 and illustrated in figs. 17 and 18. The fastest two positives in a u-quark jet carry 57% of the charged momentum, whereas only 34% is carried by the fastest two negatives. For a d-quark jet, the situation is reversed (see fig. 18); the fastest two negatives carry 52% of the charged momentum compared to 39% for the fastest two positives. These predictions should be easy to check by comparing the jets produced in $\nu p \to \mu^-$ + jet which are predominantly u-quark jets to those produced in $\bar{\nu} p \to \mu^+$ + jet which are predominantly d-quark jets.

A similar interesting and easily measured observable is the flavor of the fastest (largest-z) hadron. As table 12 shows, for a u-quark jet the fastest hadron is positive 42% of the time and negative only 20% of the time; the rest of the time, it is neutral. For a d-quark, on the other hand, the fastest hadron is positive 24% of the time and negative 34% of the time. The average charge of the fastest hadron in a u- and d-quark jet is about 0.23 and −0.10, respectively. The fastest hadron does "remember" to some extent the flavor of the quark that initiated the jet. Table 12 also shows the relatively large portion of strange particles predicted in our jets. For

Table 12
Number of times the various hadrons occured as the fastest (largest-z) particle for 10 000 quark jets with energy $P_q = 10$ GeV. Also shown are the average charge Q, third component I_3, and strangeness S of the fastest hadron

Fastest hadron	u	d	s
π^+	3194	1645	1447
π^0	2411	2462	1536
π^-	1511	2888	1356
K^+	1055	707	528
K^0	600	1062	517
K^-	466	473	2165
$\bar{K}^0$	458	458	2174
γ	305	305	277
h^+	4249	2352	1975
h^-	1977	3361	3521
h^0	3774	4287	4504
h^+/h^-	2.15	0.70	0.56
ave Q	0.227	−0.101	−0.155
ave I_3	0.191	−0.143	0.010
ave S	0.073	0.084	−0.329

a u-quark jet, the fastest hadron is a strange particle ($K^+, K^0, K^-, \bar{K}^0$) about 26% of the time.

3.5. Correlations between the fastest two charged hadrons

Although there is a considerable difference between rank in hierarchy and order in rapidity (or z), the hadrons in our jets do not completely "forget" the underlying hierarchy structure shown in fig. 1. The charge correlations between the fastest two charged hadrons, where h_1 is the fastest charged hadron and h_2 is the second fastest charged hadron and where neutrals are ignored, shown in tables 13a and 13b are a result of the underlying hierarchy structure and resonance decay effects. The combination $h_1 = +, h_2 = -$ occurs more often than $h_1 = +, h_2 = +$ and $h_1 = -, h_2 = +$ occurs more often than $h_1 = -, h_2 = -$. In fact, for a u-quark jet, the unlike sign configuration occurs almost twice as frequently as the like sign configuration. It is very unlikely for two negatives (positives) to occur as the fastest two charged particles in a u-quark (d-quark) jet (−− = 7% for a u-quark and ++ = 10% for a d-quark).

3.6. Determining the flavor of the quark

As we have seen, there are differences in the distribution of charge, total charge, fastest hadron, and correlations between the two fastest charged hadrons depending

Table 13a
Number of times various charge combinations occurred for the fastest (largest-z) two-charged hadron h_1, h_2 (h_1 = fastest charged hadron, h_2 = second fastest charged hadron) that fragmented from 10 000 quark jets with P_q = 10 GeV

h_1	h_2	u	d	s
+	+	2594	965	845
+	−	3608	3024	2743
+	none	420	102	81
+	arbitrary	6622	4091	3669
−	+	2550	3515	3648
−	−	731	1967	2193
−	none	31	287	341
−	arbitrary	3312	5769	6182
none	none	66	140	149

Same as above but $z_{h_1} \geq 0.5$

h_1	h_2	u	d	s
+	+	395	61	48
+	−	588	368	233
+	none	151	11	4
+	arbitrary	1134	440	285
−	+	264	520	474
−	−	36	226	264
−	none	4	99	84
−	arbitrary	304	845	822
none	none	8562	8715	8893

on whether the jet is initiated by a u-, d- or s-quark. The differences in the hadron charge distributions can only be seen if one has a large statistical sample of jets of one particular quark type. It is interesting to see if a criterion exists that allows one to determine the flavor of the quark jet on an event-by-event basis. Clearly, any criterion for finite-momentum jets will not work perfectly, so in order to compare the usefulness of various criteria, we define a reliability by

$$\text{reliability} \equiv (N_T - N_F)/(N_T + N_F) , \tag{3.7}$$

where N_T refers to the number of times the criterion correctly identifies the flavor of the jet from a sample containing an equal mixture of u- and d-quark jets and N_F is the number of times it is incorrect. If the criterion succeeds as often as it fails, the reliability is zero. The criterion may only apply to a sub-sample of the jets so we define an efficiency by

$$\text{efficiency} \equiv (N_T + N_F)/(\text{total number of jets}) . \tag{3.8}$$

Table 13b
Same as table 13a except that only hadrons with $z \geq 0.1$ are observed

h_1	h_2	u	d	s
+	+	1421	560	432
+	−	2006	1833	1610
+	none	2624	1205	1090
+	arbitrary	6051	3598	3132
−	+	1618	1891	1978
−	−	442	1060	1170
−	none	936	2120	2272
−	arbitrary	2996	5071	5420
none	none	953	1331	1448

Same as above but $z_{h_1} \geq 0.5$

h_1	h_2	u	d	s
+	+	158	33	12
+	−	253	225	140
+	none	723	182	133
+	arbitrary	1134	440	285
−	+	174	217	220
−	−	14	98	111
−	none	116	530	491
−	arbitrary	304	845	822
none	none	8562	8715	8893

For example, if we say that all jets where the fastest charged hadron is positive are u-quark jets and all jets where it is negative are d-quark jets, then for $P_q = 10$ GeV the reliability is about 0.25 and the efficiency is 99% (only 1% of the jets contain no charged particles). One can increase the reliability by lowering efficiency. Using the same criterion but applying it only to those jets that have one charged particle with $z \geq 0.5$ yields a reliability of 0.45 but an efficiency of only 14% *. In table 15, we list other criteria together with the reliability and efficiency for an equal mixture of u- and d-quark jets with $P_q = 10$ GeV.

* One disadvantage of the criterion which only can be applied to a small fraction of jets (low efficiency) is, of course, lower counting rate. But a much more serious difficulty is the bias introduced by not knowing experimentally the difference between a u-jet and a d-jet in the fraction of times the criterion can be applied. We could, of course, calculate these efficiency differences for our "standard" jet but we would not know whether they were right experimentally. The uncertainties are least if the efficiency is high.

Table 14
Number of times various weighted quark charge $Q_W(p)$ occured for 10 000 quark jets with energy $P_q = 10$ GeV, where $Q_W(p) = \Sigma_{i=1}^{N} z_i^p q_i$ with q_i and z_i the charge and z value of the ith hadron in a quark jet with N charged hadrons. Results are given for $p = 0.2$ and 0.5 and σ_{rms} is the root-mean-square deviation from the mean.

	Weighted charge	u	d	s
$p = 0.2$	$Q_W \geq 0$	7197	3499	3322
	$Q_W < 0$	2737	6361	6529
	$\langle Q_W \rangle$	0.39	−0.25	−0.27
	σ_{rms}	0.68	0.66	0.67
$p = 0.5$	$Q_W \geq 0$	7172	3601	3320
	$Q_W < 0$	2762	6259	6531
	$\langle Q_W \rangle$	0.26	−0.15	−0.18
	σ_{rms}	0.43	0.42	0.41
Same as above but observe only hadrons with $z \geq 0.1$				
$p = 0.2$	$Q_W \geq 0$	6172	3482	3045
	$Q_W < 0$	2875	5187	5507
	$\langle Q_W \rangle$	0.34	−0.19	−0.26
	σ_{rms}	0.76	0.77	0.75
$p = 0.5$	$Q_W \geq 0$	6168	3486	3039
	$Q_W < 0$	2879	5183	5513
	$\langle Q_W \rangle$	0.24	−0.14	−0.18
	σ_{rms}	0.52	0.53	0.51

From table 15, one sees that none of the first fourteen criteria listed gives a very high reliability while still maintaining a reasonable efficiency. This is because the rank in hierarchy and the order in momentum are considerably mixed up as discussed earlier and witnessed by table 11. The highest reliability with a large efficiency is obtained by assigning jets with total charge $Q > 0$ as u-quark jets and jets with $Q < 0$ as d-quark jets. The reliability is 0.45 with a 66% efficiency. Unfortunately, the total charge on a quark jet is not easily measured since it depends on including all the forward moving low-momentum hadrons which are difficult to measure without also including background from other sources. A quantity easy to measure experimentally is the total charge of all those hadrons in the jet which have $z \geq 0.1$. The reliability, however, now decreases to 0.38. If one wants to apply this criterion to all the events with $Q = 0$ jets assigned as d type, then the reliability decreases even further to 0.26 (number 8 in table 15).

The mean total charge of a large momentum u-jet is 0.60 and a d-jet is −0.40 differing by 1.0. This would seem to permit a clear separation of these jets. However, even with a jet of extreme momentum, the total charge Q of all hadrons of $P_z > 0$

Table 15
Various criterion for determining the flavor of the quark initiating the jet for an equal mixture of $P_q = 10$ GeV u- and d-quark jets together with the reliability = (true−false)/(true+false), where "true" refers to the number of times the criterion succeeded in selecting the correct flavor and "false" to the number of times the criterion failed. The efficiency is the number of jets (true+false) to which the criterion can be applied divided by the total number of jets generated.

Criterion	Reliability	Efficiency
1. fastest hadron positive ⇒ u-jet fastest hadron negative ⇒ d-jet	0.27	60%
2. fastest charged hadron positive ⇒ u-jet fastest charged hadron negative ⇒ d-jet	0.25	99%
3. charged hadron with $z \geq 0.5$ is positive ⇒ u-jet charged hadron with $z \geq 0.5$ is negative ⇒ d-jet	0.45	14%
4. fastest two charged hadrons are both positive ⇒ u-jet fastest two charged hadrons are both negative ⇒ d-jet	0.46	31%
5. total charge of jet $Q > 0$ ⇒ u-jet total charge of jet $Q < 0$ ⇒ d-jet	0.45	66%
6. same as 5 but only observe hadrons with $z \geq 0.1$	0.38	62%
7. total charge of jet $Q > 0$ ⇒ u-jet total charge of jet $Q \leq 0$ ⇒ d-jet	0.33	100%
8. same as 7 but only observe those hadrons with $z \geq 0.1$	0.26	100%
9. for $N_{ch} = 1$ jets $Q > 0$ ⇒ u-jet for $N_{ch} = 1$ jets $Q < 0$ ⇒ d-jet	0.68	4%
10. for $N_{ch} = 3$ jets $Q > 0$ ⇒ u-jet for $N_{ch} = 3$ jets $Q < 0$ ⇒ d-jet	0.47	13%
11. for N_{ch} = odd jets $Q > 0$ ⇒ u-jet for N_{ch} = odd jets $Q < 0$ ⇒ d-jet	0.40	50%
12. same as 9 but only observe hadrons with $z \geq 0.1$	0.38	34%
13. same as 10 but only observe hadrons with $z \geq 0.1$	0.31	15%
14. same as 11 but only observe hadrons with $z \geq 0.1$	0.36	50%
15. "weighted" charge $Q_W(p = 0.2) \geq 0$ ⇒ u-jet "weighted" charge $Q_W(p = 0.2) < 0$ ⇒ d-jet (see eq. (3.9))	0.37	99%
16. "weighted" charge $Q_W(p = 0.5) \geq 0$ ⇒ u-jet "weighted" charge $Q_W(p = 0.5) < 0$ ⇒ d-jet	0.36	99%
17. same as 15 but only observe hadrons with $z \geq 0.1$	0.28	89%
18. same as 16 but only observe hadrons with $z \geq 0.1$	0.28	89%
19. "weighted" charge $Q_W(p = 0.2) \geq 0.4$ ⇒ u-jet "weighted" charge $Q_W(p = 0.2) < -0.3$ ⇒ d-jet	0.51	63%
20. "weighted" charge $Q_W(p = 0.5) \geq 0.4$ ⇒ u-jet "weighted" charge $Q_W(p = 0.5) < -0.3$ ⇒ d-jet	0.58	46%
21. same as 19 but only observe hadrons with $z \geq 0.1$	0.38	62%
22. same as 20 but only observe hadrons with $z \geq 0.1$	0.40	55%

must be an integer and thus a random variable. There is an unavoidable noise depending on whether a particular charged particle in the plateau happens to have P_z greater or less than zero. Even though the plateau is neutral and all the difference of u- and d-quark jets lies far away at higher z, one is trying to sum a long series like +1−1+1+1−1 +1−1−1... not knowing where to stop, but knowing only that +1 and −1 become more and more equally likely to occur as we go further down the series (to lower z). The proper thing to do is, of course, the analogue of Abel summation, weigh the terms with a gradually decreasing weight as we go down the series. If the weight falls gradually enough from unity at the beginning, the excess charge there will be accurately picked up. However, the random ±1 far down where the weight has fallen toward zero will produce no fluctuations. That is, if particle i has "z rapidity" Y_{z_i} and charge q_i, we form the "weighted" charge

$$Q_W(p) = \sum_i q_i \exp(-pY_{z_i}) = \sum_i z_i^p q_i \,, \tag{3.9}$$

where p is a small number. This quantity will have a mean (close to $\langle Q\rangle$ as $p \to 0$) distinct for u- and d-quark jets. Furthermore, the "noise" or fluctuations expected from having to stop the sum below some finite $z_{\min}$ is $\pm z_{\min}^p$ which can be made small as long as $z_{\min}$ can be made small enough.

For a given experimental circumstance, however, $z_{\min}$ is fixed and the criteria that p be small and that $z_{\min}^p$ also be small are opposed. For sufficiently small $z_{\min}$ there is no problem, but because of the wide fluctuations in rapidity that the particles in our model suffer, we have found that in practice the method does not work as well as we hoped. For $z_{\min} = 0.1$, with $p = 0.5$, for example, the fluctuating uncertainty $z_{\min}^p$ is 0.3 times less than the gross sum $Q = \Sigma q_i$; but such a large p means that $Q(P)$ does not average as large as $\langle Q\rangle$. Even worse is that for such a large p the contributions of high-z particles depend so strongly on the precise z value they actually have.

Figs. 20 and 21 show the distribution of $Q_W(p)$ with $p = 0.2$ and 0.5, respectively, for a u- and d-quark jet of energy $P_q = 10$ GeV (including all hadrons with $P_z > 0$). The $p = 0.2$ distributions are considerably broader than the $p = 0.5$ case; however, the former has mean values $\langle Q_W\rangle$ that are more widely separated ($\langle Q_W\rangle_u - \langle Q_W\rangle_d = 0.64$ for $p = 0.2$ and only 0.41 for $p = 0.5$). In both cases, there is a clear separation of the u- and d-jets. By the use of table 14, we find a reliability of 0.37 if we assign jets with $Q_W \geqslant 0$ as u-quark type and those jets with $Q_W < 0$ as d-quark type with $p = 0.2$. The efficiency of this criterion is excellent (99% since we include only those jets with at least one charged hadron). One can obtain a higher reliability (but lower efficiency) by excluding from consideration those jets with Q_W values occurring in the overlap region of the u- and d-quark jet distributions. For example, table 15 shows that if we assign jets with $Q_W \geqslant 0.4$ as u-type and those with $Q_W < -0.3$ as d-type, then for $p = 0.5$ we get a 58% reliability with 46% efficiency. This "weighted" charge technique gives us better reliability factors than the

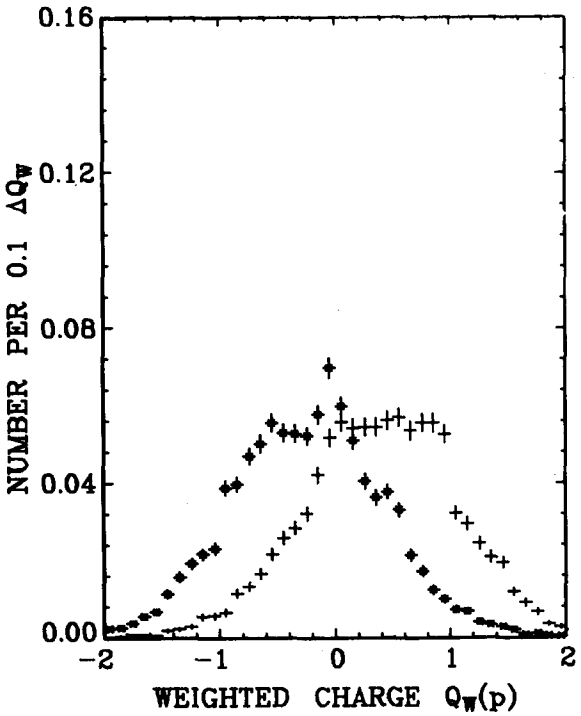

Fig. 20. Predicted distribution of weighted quark charge $Q_W(p)$ for a u- (+) and d-quark (X) jet with P_q = 10 GeV, where $Q_W(p) = \Sigma_{i=1}^{N} z_i^p q_i$ with z_i and q_i being the z value and charge of the ith hadron and where the sum is over all hadrons in the jet with $p_z \geq 0$. The value of the power p is taken to be 0.2. a = 0.77, $\alpha_{ps} = \alpha_v$ = 0.5. d-quark, $\langle Q_W \rangle = -0.25$; u-quark, $\langle Q_W \rangle = 0.39$.

other criterion in table 15. Nevertheless, even a reliability of 58% (about 4 out of 5 correct) is not too impressive.

In practice, for hadron-induced jets, it might be possible to go to lower z_{min}, perhaps even to p_z somewhat negative, allowing a smaller p value. The many "background" particles from the longitudinal jets may perhaps not contribute to much noise. But data from lepton jets should ultimately determine the best parameter p, z_{min} and criterion to use.

In view of the small reliability factors in table 15, we must conclude that our efforts to find a method of determining the quark flavor of a jet on an event-by-event basis have failed for jets of energy $P_q \lesssim 10$ GeV. The criterion can be made more reliable only with much higher momentum jets. (The method of "weighted" charge becomes an exact separation at very high momenta.) Nevertheless, table 15 is useful in summarizing the differences between u- and d-quark jets.

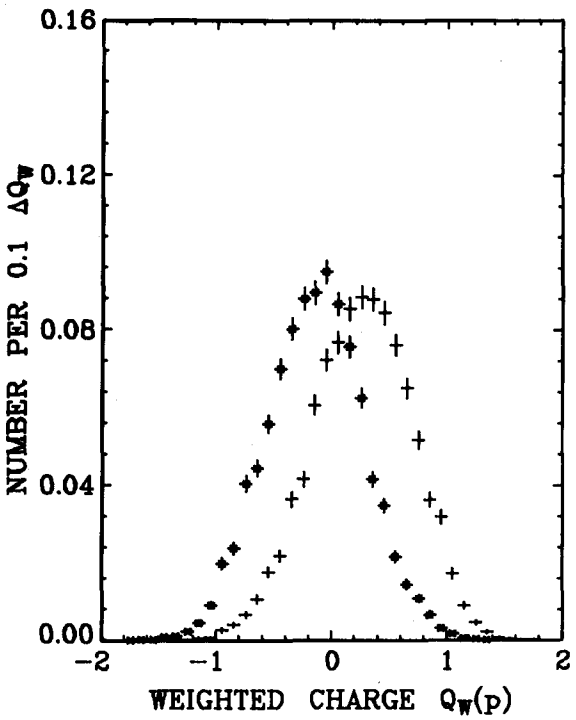

Fig. 21. Same as fig. 20 but where the power p is taken to be 0.5. d-quark, $\langle Q_W \rangle = -0.15$, u-quark, $\langle Q_W \rangle = 0.26$.

4. Properties of the quark rapidity plateau

4.1. Rapidity correlations

4.1.1. Correlations between adjacent-rank mesons

There are two sources of correlations in our model. Naturally, there is the correlation among secondary particles that are the decay products of the same primary meson. In addition, however, the primary mesons are not formed at random in rapidity. Primary mesons adjacent in rank are correlated in both flavor and rapidity since they each contain a quark (or antiquark) that came from the same $q\bar{q}$ pair. The two primary mesons of adjacent rank tend to occur near each other in rapidity, Y_z, as shown in fig. 22. The mean $|\Delta Y_z|$ between mesons adjacent in rank is about 1.8 units, where all the decay products of a particular primary meson are assigned the rank of that meson (see fig. 1). Fig. 22 also shows the distribution of $|\Delta Y_z|$ between mesons with the same rank ($\langle |\Delta Y_z| \rangle = 0.9$). All flavor correlations in the quark jets occur between primary mesons of adjacent rank. The flavor of a meson

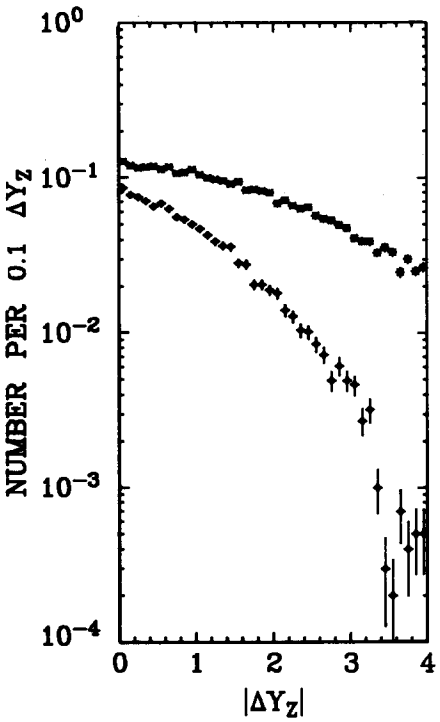

Fig. 22. The distribution of distances ΔY_Z between the hadrons coming from one primary and those coming from another primary next in rank ×, $\langle |Y_Z| \rangle = 1.8$. The distribution ΔY_Z among the secondary hadrons which come from the decay of a single primary ◇, $\langle |Y_Z| \rangle = 0.9$. $a = 0.77$, $\alpha_{ps} = \alpha_v = 0.5$.

of rank $r + 2$ is independent of the flavor of the meson of rank r. Rank is not a physical observable; however, the correlations shown in fig. 22 do produce effects in certain physical observables which we now proceed to examine.

4.1.2. Rapidity-gap distributions [16]

Figs. 23 and 24 show the distribution of Y_Z gaps between all particles, charged particles, and positive particles (equals negative particles) before and after decay in the rapidity plateau *. Because two primary mesons of adjacent rank have net charge either ±1 or zero, small ΔY_Z gaps occur more frequently between charge

* In order to avoid biasing against large Y_Z gaps, the distributions in figs. 23, 24 and 25 are calculated by first ordering all particles in Y_Z with $Y_{Z_{i+1}} > Y_{Z_i}$ and then considering all Y_{Z_i} in the range $3.0 < Y_{Z_i} < 6.0$ *but* when forming the gap length $\Delta Y_{Z_i} = |Y_{Z_i} - Y_{Z_{i+1}}|$, $Y_{Z_{i+1}}$ is allowed the range $3.0 < Y_{Z_{i+1}} < 9.0$. Then only gaps $\Delta Y_{Z_i} < 3.0$ are displayed. This method requires a rapidity interval *twice* as large as the maximum gap one decides to plot.

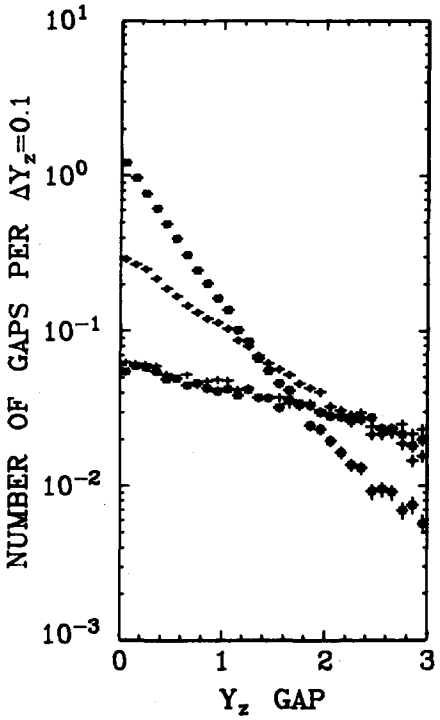

Fig. 23. Predicted number of times various Y_z gaps occur between all primary mesons, between charged primaries and between positive primaries (the same as for negative primaries) in the rapidity plateau of a u-quark jet *before* the primary mesons are allowed to decay. $a = 0.77$, $\alpha_{ps} = \alpha_V = 0.5$. □ all, ◇ charged, + positives, x negatives.

mesons (due to +–) than between negative mesons. For large Y_z gaps, the situation is reversed and there are more large Y_z gaps between the negatives than between the charged mesons. (Note that a gap between negatives can contain positives or neutrals whereas a gap between charged particles can only contain neutrals.)

The distribution of Y_z gaps carrying a specific charge is shown in fig. 25, where

$$Q_k = \sum_{i=1}^{k} q_i - q_0 \tag{4.1}$$

is the charge carried by the kth Y_z gap and q_i is the charge of the ith meson (ordered in Y_z). The quantity q_0 is the charge of the quark that initiated the jet (u-quark in fig. 25). If the mesons were ordered in hierarchy, only the net charge, $\Sigma_{i=1}^{k} q_i$, equal to one or zero could be obtained for a u-quark jet; Q_k must be the charge of an anti-quark. For ordering in Y_z, other values of $\Sigma_{i=1}^{k} q_i$ can occur, but only by mixing up hierarchy order and Y_z order. Because of this, for a u-jet, gaps of charge $-\frac{2}{3}$ and $\frac{1}{3}$

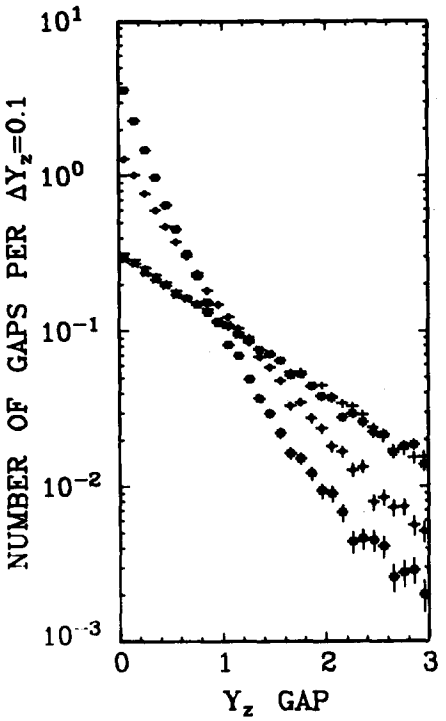

Fig. 24. The same as fig. 23 but *after* the vector mesons (and the η and η') have decayed according to the particle tables.

dominate at large gaps over the other gap charges *. (The distribution of $Q = -\frac{2}{3}$ and $Q = \frac{1}{3}$ gaps are equal, as are gaps of charge $Q = \frac{4}{3}$ and $Q = -\frac{1}{3}$, etc.)

4.1.3. Charged particle correlations

In analogy with the statistical-mechanical description of density fluctuations in a liquid, one defines a correlation function (see, for example, ref. [17])

$$C(Y_1, Y_2) = \frac{1}{\sigma}\frac{\mathrm{d}^2\sigma}{\mathrm{d}Y_1\,\mathrm{d}Y_2} - \frac{1}{\sigma^2}\frac{\mathrm{d}\sigma}{\mathrm{d}Y_1}\frac{\mathrm{d}\sigma}{\mathrm{d}Y_2} . \tag{4.2}$$

The "correlation moment", f_2, is related to it by

$$f_2 = \int \mathrm{d}Y_1\,\mathrm{d}Y_2\, C(Y_1, Y_2) = \langle N(N-1)\rangle - \langle N\rangle^2 . \tag{4.3}$$

* In an exchange picture like that discussed by Pirilä, Thomas and Quigg in ref. [16], large gaps with charge $-\frac{2}{3}$ and $\frac{1}{3}$ correspond to the (allowed) exchange of a $\bar{u}$- and $\bar{d}$-quark, respectively, whereas the other gap charges correspond to lower-lying (exotic-type) exchanges. Hence the former, with a higher intercept ($\frac{1}{2}$), is expected to dominate at large gaps as it does.

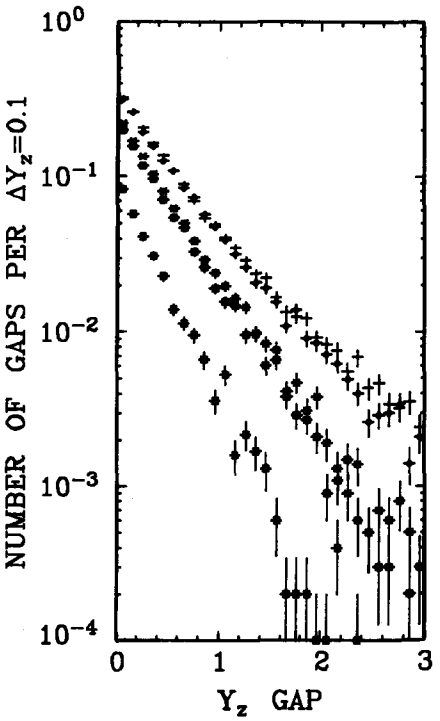

Fig. 25. Predicted number of times various *charged* Y_z gaps occur for a u-quark jet (after decay) where the charge of the kth gap is given by $Q_k = \Sigma_{i=1}^{k} q_i - q_0$, where q_i is the charge of the ith hadron (ordered in Y_z) and q_0 is the charge of the initiating quark (in this case $q_0 = \frac{2}{3}$). $a = 0.77$, $\alpha_{ps} = \alpha_v = 0.5$. $\diamond\ Q = -\frac{2}{3}$, $+\ Q = \frac{1}{3}$, $\times\ Q = \frac{4}{3}$, $\square\ Q = -\frac{1}{3}$, $*\ Q = -\frac{4}{3}$.

In addition, one can define a "normalized" correlation function by

$$R(Y_1, Y_2) = C(Y_1, Y_2) \Big/ \frac{1}{\sigma^2} \frac{d\sigma}{dY_1} \frac{d\sigma}{dY_2} . \tag{4.4}$$

In the absence of any dynamical correlations, the probability to observe in a single jet one hadron at rapidity Y_1 and a second hadron at rapidity Y_2, together with anything else, would be equal to the product of the probabilities to find hadrons at rapidity Y_1 and Y_2 in different jets and (4.2) would vanish. Figs. 26 and 27 show the value of $C(Y_{z_1}, Y_{z_2})$ and $R(Y_{z_1}, Y_{z_2})$, respectively, for a negative hadron at $Y_{z_1} = 4.0$ and a positive (upper) and negative (lower) hadron at Y_{z_2} *versus* $\Delta Y_z = Y_{z_1} - Y_{z_2}$. The region $-2 \leqslant \Delta Y_z \leqslant 2$ is the plateau region and $2 \leqslant \Delta Y_z \leqslant 4$ is the "end of the quark" region as can be seen from fig. 8. Also shown are the analytic results for the case where no particles decay (in this case, the analytic method is exact). Resonance decay clearly plays an important role in correlations; however, in

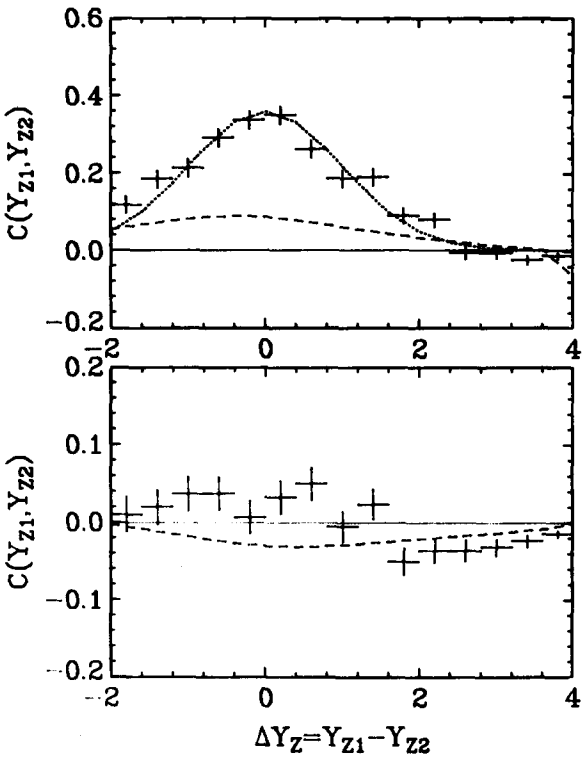

Fig. 26. Predicted behavior of the two-particle correlation function $C(Y_{z_1}, Y_{z_2})$ defined by (4.2) where $Y_{z_1} = 4.0$ and we have plotted *versus* $\Delta Y_z = Y_{z_1} - Y_{z_2}$. Results are given for h_1 negative and h_2 positive (upper) and h_1 negative and h_2 negative (lower) and are generated using Monte Carlo (points). The dashed curves are the results for $C(Y_{z_1}, Y_{z_2})$ *before* the primary mesons are allowed to decay. The dotted curve (to guide the eye) is $0.36 \exp(-\frac{1}{2}(\Delta Y_z)^2)$. $a = 0.77$, $\alpha_{ps} = \alpha_v = 0.5$, $Y_{z_1} = (4.0, 4.4)$.

our model there is some clustering of the primary mesons before decay. The final correlation function (after decay) $C(Y_1, Y_2)$ for oppositely charged hadrons shows the characteristic short-range correlation behavior [16–19] roughly like $\exp(-(\Delta Y_z)^2/4\delta^2)$ with a correlation length, 2δ, of about 1.4. The correlation between two negatives is, on the other hand, quite small. The "correlation moment" f_2 in (4.3) after decay is given in table 3 and for ++ and −− it is negative.

4.1.4. Mass distribution

The distribution of two-particle mass for u-quark jets of $P_q = 10$ GeV resulting from the model is shown in figs. 28 and 29. One can see the ρ^0 and K^{*+} in the $\pi^+\pi^-$ and $K^+\pi^0$ combinations (our resonances have zero mass width). If our estimate of

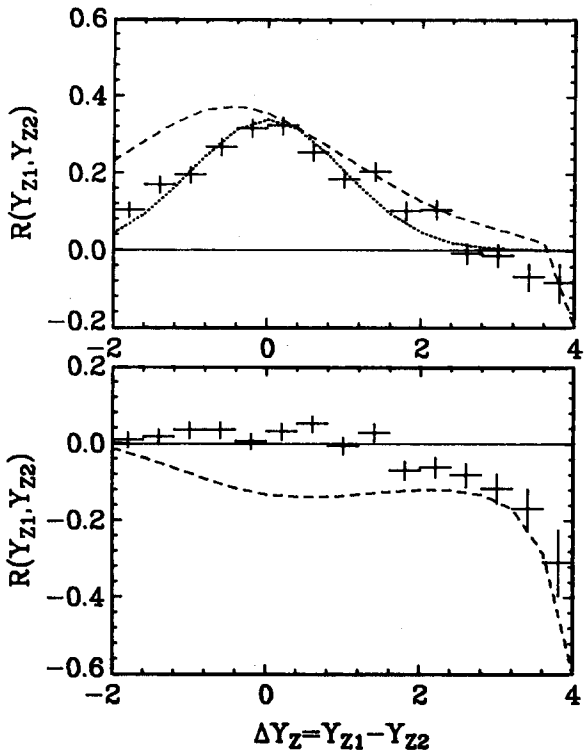

Fig. 27. Same as fig. 26 but for the "normalized" correlation function defined in (4.4). The dotted curve (to guide the eye) is $0.34 \exp(-\frac{1}{2}(\Delta Y_z)^2)$.

the resonance contributions is roughly correct, then one would expect to see such resonances in the jets produced in lepton- or hadron-initiated processes.

4.2. Comparison with pp collisions

Many of the features predicted by our model for the behavior of the quark rapidity plateau are similar to those observed for the low-$p_\perp$ rapidity plateau generated in proton-proton collisions. The rapidity gap distributions, +− charged correlations, mass distributions, and charged multiplicities are quite similar to that seen in pp interactions. Similarities between the plateau behavior in lepton and low-$p_\perp$ hadron experiments have often been noted [20]. It will be interesting to see experimentally if they are really very much alike and to study theoretically why this may (or may not) be so.

In making this comparison, one must be careful of the contributions from diffrac-

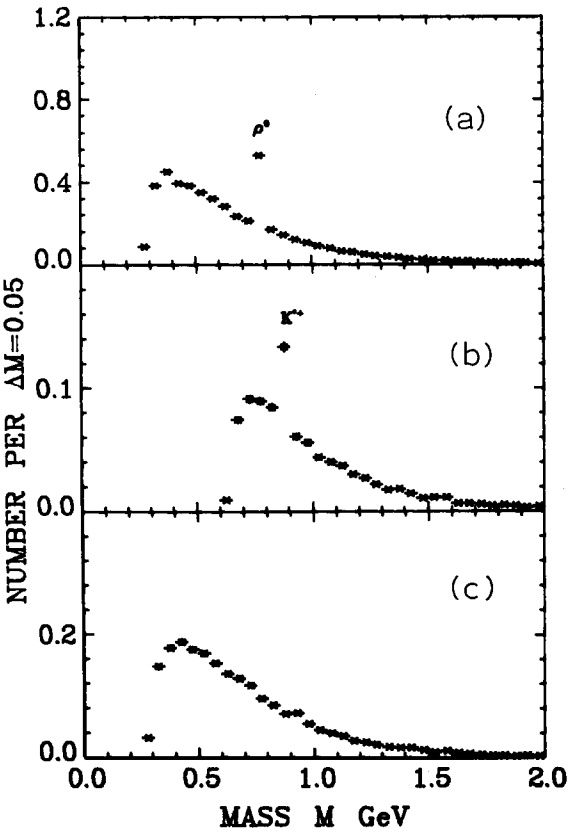

Fig. 28. Plot of the two-particle mass of (a) $\pi^+\pi^-$, (b) $K^+\pi^0$, and (c) $\pi^+\pi^+$ from a u-quark jet with $P_q = 10$ GeV from our jet model with $a = 0.77$, $\alpha_{ps} = \alpha_v = 0.5$. (Note that our resonances have zero width.)

tive events in pp collisions which have no counterpart in the quark jets. The comparison should properly be made only with the inelastic non-diffractive part of pp collisions (if that can actually be defined and separated out). One place where this diffractive component plays an important role is in the behavior of f_2^-. In pp collisions, f_2^- becomes positive as the negative particle multiplicity $\langle N_- \rangle$ increases (i.e., as the energy of the collision is increased). On the other hand, our model for quark jets predicts a negative f_2^- for $P_q \lesssim 500$ GeV (see table 3) and recent data on νp interactions, where the model should apply, indicate that it is indeed negative [21]. For those $p\bar{p}$ annihilation events which contain no final baryons so diffraction plays no role f_2^- is also negative.

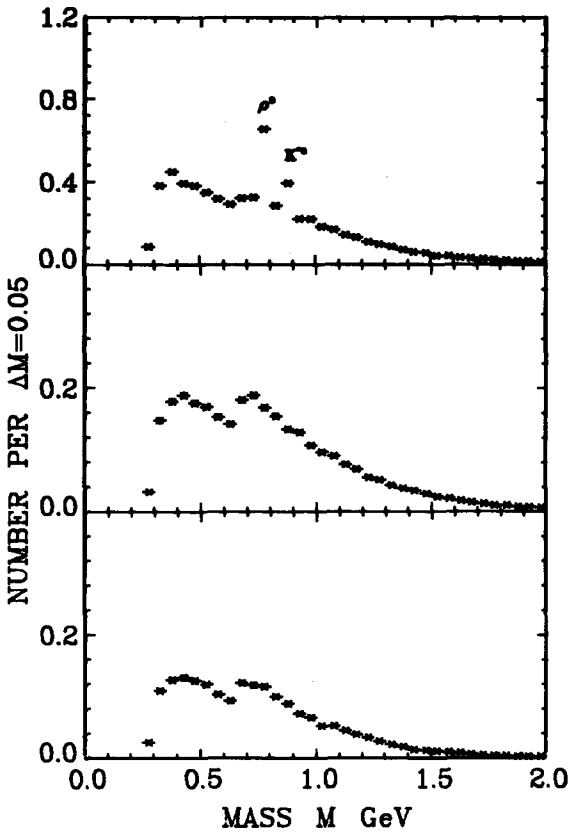

Fig. 29. Same as fig. 28 but for (a) h^+h^-, (b) h^+h^+, and (c) h^-h^-, where $h = \pi + K$.

4.3. *Problems with the model*

There is, of course, the obvious problem that the model contains no protons or other baryons and is thus incomplete. They might be included in the same framework if we were to consider that the field which makes the quark-antiquark pairs could, from time to time, make pairs of diquarks (two quarks whose color is in a $\bar{3}$ representation) and anti-diquarks. To implement this idea, however, requires inventing a few new functions and parameters which we have too little information at present to guess. Since baryons are probably not produced with great frequency in quark jets, neglecting them probably causes no serious modifications of the meson distributions. Of course, we cannot predict baryon distributions at all.

In addition, we have not included quantum effects. We have dealt solely with probabilities and not amplitudes. It would be interesting to imagine the recursive

principles to apply to amplitudes instead of probabilities. Instead of (2.3), one would write

$$\sqrt{\gamma_a}\sqrt{\gamma_b}\sqrt{\gamma_c}\ldots\prod_i \phi(\eta_i) \tag{4.5}$$

as the amplitude to find primary mesons with a set of flavors and momenta, where $\phi(\eta)$ is a (possibly complex) amplitude whose absolute square is $f(\eta)$. By adding amplitudes in the appropriate manner, allowance would then be made for the Bose nature of indistinguishable primary mesons.

The most serious problem with the model is that it suffers from a defect in principle. As Casher, Kogut and Susskind have pointed out [10], the correct way to look at the development of these jets is from the center out, not from each end in toward the center. That is, as the original quarks' rapidities separate in, say, an e^+e^- experiment, the first new quark pairs are made at relatively small momenta, then the quarks leaving the new pair generate a new pair between them, etc. We have not been able to develop a simple ansatz for both flavor and momentum distributions in accord with this idea. Instead, our ansatz thinks of the first pair forming near one end of the momentum chain, and then further ones follow generally down the momentum scale. This mechanism has been well refuted by Bjorken and Kogut and Susskind. Our first surprise from the "chain-decay" point of view is that the function, $zf(1-z)$, in (2.21) giving the momentum distribution of the first primary meson must be so peaked toward *low* momentum, z, to agree with experiment. It is not clear how the leading quark manages to find itself so far down in momentum.

We can also see that something is wrong in principle with the chain-decay ansatz by considering the nature of the plateau region for an energetic $q\bar{q}$ pair produced in an e^+e^- colliding beam experiment. We have argued that this plateau region could be analyzed by going far down in rapidity in the jet from the quark q; even so far down that the hadrons are, in fact, moving slightly backwards (i.e., in the direction of $\bar{q}$). If this is true, then all properties of this region would have to be the same if analyzed (in reverse order) as a property of the $\bar{q}$-jet. Measure rapidities in the c.m.s. so the quark q has rapidity Y_0 and the antiquark $-Y_0$. We first ask in the q-system, what is the probability that three primary mesons adjacent in hierarchy are located at rapidities Y_1, Y_2, and Y_3 (per dY_1, dY_2, dY_3). This function $K(Y_0 - Y_1, Y_0 - Y_2, Y_0 - Y_3)$ deep in the plateau region depends only on rapidity differences, and not on Y_0 (i.e., it equals a function $L(Y_2 - Y_1, Y_3 - Y_2)$). Now seen in the other direction as a $\bar{q}$ jet, the three primary mesons are in rank 3, 2, 1 and the rapidity distance from the end of $\bar{q}$ are $Y_0 + Y_3$, $Y_0 + Y_2$, and $Y_0 + Y_1$. Calculating in this way, we have $K(Y_0 + Y_3, Y_0 + Y_2, Y_0 + Y_1)$ and, therefore, $L(Y_3 - Y_2, Y_2 - Y_1)$. Choosing $Y_2 = 0$, $Y_1 = \ln \xi$, and $Y_3 = -\ln \eta$ so that the three particles are in the $E + p_z$ ratio ξ, 1, $1/\eta$ (or seen in the reverse order $E - p_z$ ratio η, 1, $1/\xi$), we should have

$$L(-\ln \xi, -\ln \eta) = L(-\ln \eta, -\ln \xi)\,, \tag{4.6}$$

if the theory were truly symmetrical.

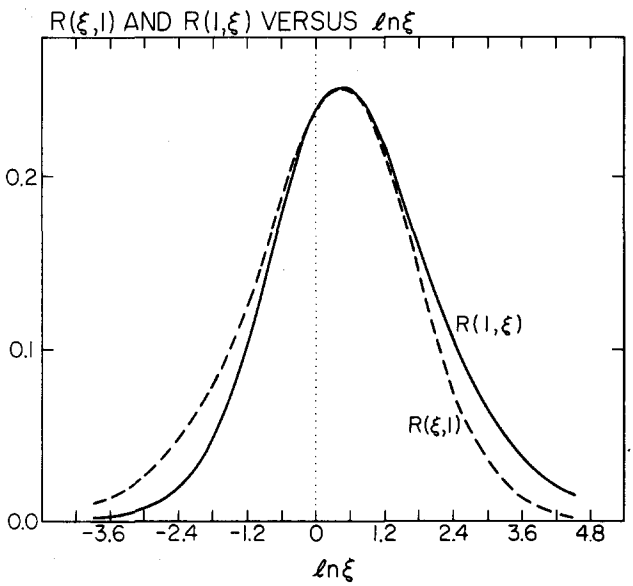

Fig. 30. Illustration of the asymmetry in our model of functions $R(\xi, \eta)$ describing correlations among three primaries adjacent in rank in the plateau (discussed in subsect. 4.3). The curves are $R(1, \xi)$ (solid) and $R(\xi, 1)$ (dashed) *versus* ln ξ. They were calculated using $f(\eta) = 3\eta^2$. Theoretically, $R(\xi, \eta)$ should be a symmetric function.

Direct calculation of the function $L(-\ln \xi, -\ln \eta)$, which we write as $\xi\eta R(\xi, \eta)$ so R is the number of particles per $d\xi\, d\eta$, shows it is *not* symmetrical. The difference between $R(\xi, \eta)$ and $R(\eta, \xi)$ is not great, yet that there is any difference at all shows our physical view is not entirely sound. The difference is illustrated in fig. 30, where we choose $\eta = 1$ and compare $R(\xi, 1)$ and $R(1, \xi)$ calculated for the simple case $f(\eta) = 3\eta^2$. The differences for other values of η are similar or not as large. Since rank in hierarchy is not physically observable, neither is $R(\xi, \eta)$. However, any amount of asymmetry of $R(\xi, \eta)$ will result in an observable (in principle) asymmetry in the rapidity plateau for three hadrons whose flavors are such that they *could* occur adjacent in rank (e.g., K^+, K^-, π^+). These asymmetries are quite small. None the less, they represent a defect of the model.

We have found the "chain-decay" ansatz so simple to formulate and to analyze arithmetically and analytically that we wanted to study it as a possible approximation by which we might get a rough idea of the general behavior of quark jets. It is important to have such a scheme to make some suggestions for the planning and design of "jet" experiments. It is delightful that so few assumptions will yield a jet model which is so complete in being able to describe a jet. (Only the transverse momentum correlation questions are unanswered.)

5. Transverse-momentum results

5.1. Transverse-momentum distributions versus z, Y, and M^2

The *mean* distribution of transverse momentum depends in no way on our assumed correlations between primary mesons. None of the details of our recursive scheme are of much concern; just the distribution in z, $F(z)$, of primary mesons and the assumption that all the *primary* mesons are distributed in transverse momentum in the same way (which we take to be a Gaussian as eq. (2.46) independent of z, flavor or spin). In our previous work (FFF), we assumed that all the *final* mesons (direct plus indirect) were distributed the same, independent of z. Our newer view, that it is the *primary* mesons which have the universal distribution in transverse momentum, produces a number of interesting effects which we will now discuss.

The transverse momentum of the final mesons has two components: the original momentum $P_\perp$ of the primary mesons plus the additional $Q_\perp$ received by the products of those primary mesons that decay. Assuming that half of the primary mesons are vectors that decay and letting the η and η' also decay, we can easily calculate the mean transverse momentum expected for various particles in the jet. As discussed in subsect. 2.7.2, we find that using $\sigma = 350$ MeV in (2.48) produces a mean transverse momentum of charged pions of $\langle k_\perp \rangle_\pi = 323$ MeV. The mean transverse momentum of the primaries (2.48) is then 439 MeV, considerably larger than that of the secondaries *.

The reason for this can be seen in the coordinate system boosted so that the z component of the primary meson is zero. It does have a $p_\perp$, however. If it is of mass M and disintegrates into two mesons each of mass $\frac{1}{2}M$ (so that the Q value is zero), then these decay products have only $\frac{1}{2}p_\perp$. Thus disintegrations considerably reduce the effect of $p_\perp$. The mean value of $Q_\perp$ generated by a spherical distribution of maximum momentum Q if $p_\perp = 0$ is $\frac{1}{4}\pi Q$, but the values of Q from the particle tables are not so large as 400 MeV on the average. Of course, there are mutual effects when both $p_\perp$ and Q are non-zero but the qualitative effect is clear; the large $\langle p_\perp \rangle$ of the primaries is decreased by observing the mean $\langle k_\perp \rangle$ of the final mesons. Even though some primaries do not decay and thus contribute directly to $\langle k_\perp \rangle$, in averaging over all particles the indirect mesons (decay products) have more weight for they occur more frequently. In addition, because more of the decay products of the vector mesons (and $\eta + \eta'$) are pions than kaons, the transverse-momentum distribution of kaons resembles more closely the distribution of primaries than does the pion distribution. The latter distribution is more sharply peaked at small $k_\perp$, as shown in fig. 31. The mean $k_\perp$ for final pions is

$$\langle k_\perp \rangle_{\pi^\pm} = 323 \text{ MeV}, \tag{5.1a}$$

whereas for final kaons, it is

* This has been pointed out by Seiden in ref. [13].

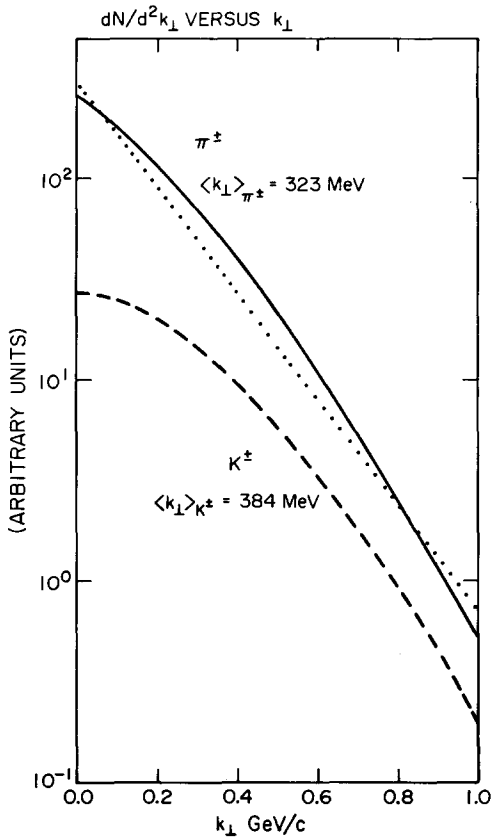

Fig. 31. Distribution of transverse momentum, $dN/d^2k_\perp$ *versus* $k_\perp$ for $\pi^\pm$ and $K^\pm$ resulting from a u-quark jet in our model with $a = 0.77$, $\alpha_{ps} = \alpha_v = 0.5$ and $\sigma = 350$ MeV. The dotted straight line is $\exp(-6k_\perp)$.

$$\langle k_\perp \rangle_{K^\pm} = 384 \text{ MeV} . \tag{5.1b}$$

Almost all the rho mesons are direct so that

$$\langle k_\perp \rangle_\rho = 439 \text{ MeV} , \tag{5.1c}$$

which is the same as the distribution of primary mesons. The mean $k_\perp$ of all the final particles is very close to that for pions since 75% of the final particles are pions. The exact shapes of the transverse-momentum distributions shown in fig. 31 depend on our arbitrary assumption of a Gaussian distribution for the primaries (2.46). The tendency for higher-mass particles like the K or ρ to have a flatter distribution in $k_\perp$ and a larger $\langle k_\perp \rangle$ than the lighter π mesons is observed in the plateau region of ordinary pp collisions. In our model, the reason is not directly

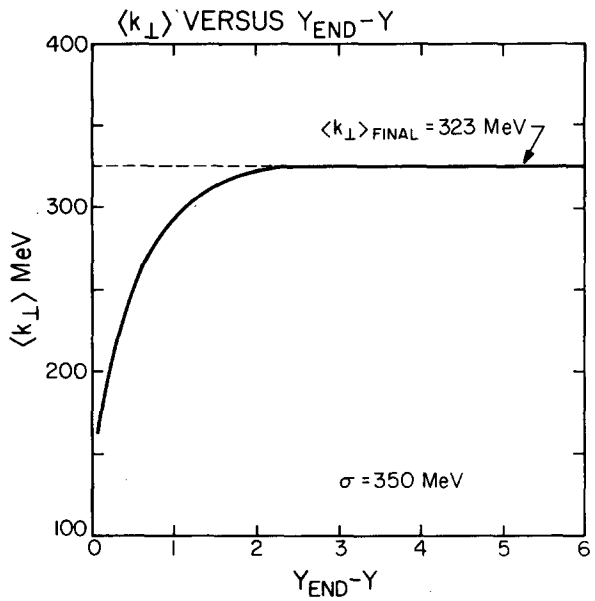

Fig. 32. The mean value of the transverse momentum of all hadrons, $\langle k_\perp \rangle$, *versus* $Y_{\text{end}} - Y$, where Y_{end} is as in fig. 11.

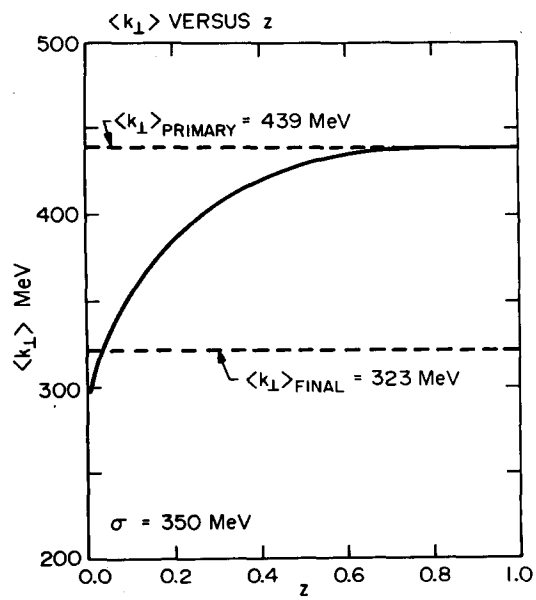

Fig. 33. The mean value of the transverse momentum of all hadrons, $\langle k_\perp \rangle$, *versus* z. Also shown by dashed lines are the total mean $k_\perp$ (summing over all z) of the primary mesons before decay (439 MeV) and after decay (323 MeV).

due to the K and ρ being more massive than the π, but because a smaller fraction of them are due to resonance decays than for the π.

How is the transverse momentum distributed in rapidity Y and in z? We see from fig. 32 that $\langle k_\perp \rangle$ for particles of a given rapidity Y, in the plateau region, and well toward the forward direction where the number of particles begins to fall off, have the mean $k_\perp$ of 323 MeV as in (5.1a). Only the few particles in the large-Y region (near Y_{end}) have $\langle k_\perp \rangle$ smaller than 323 MeV. On the other hand, particles with a given z have a mean $k_\perp$ which depends on z as shown in fig. 33. For $z \gtrsim 0.1$, $\langle k_\perp \rangle$ is larger than 323 MeV and approaches the mean of the primary mesons, 439 MeV, as z approaches one.

This latter behavior is obvious since only primary mesons can obtain a z value very near one. However, the reason $\langle k_\perp \rangle$ for particles with z in the range 0.2–0.6 is so large requires further discussion. Consider a primary meson generated at some z_0 (and true rapidity Y_0), but look at it in the frame for which it has zero longitudinal momentum p_z. First, suppose its original perpendicular momentum, $p_\perp$, is zero and suppose it decays into two mesons. Then the secondaries acquire with equal likelihood both positive and negative z component of momentum Q_z; that is, both positive and negative rapidity. Thus, back in the lab system (just add a constant Y), the secondaries are found symmetrically spread in rapidity about the original rapidity Y_0 of the parent. It is otherwise with z, the secondaries are widely spread in z but only over values below z_0 (uniformly from 0 to z_0 for massless products, for example).

Now to see what happens if the parent meson has non-zero $p_\perp$, imagine this $p_\perp$ to arise from a very small rotation of the original large p_z (by an angle $p_\perp/p_z$). It is clear that if a product ends up at a momentum p_{z_1}, its share of the parent $p_\perp$ is only $(p_{z_1}/p_z)p_\perp$, or fractionally z/z_0 of the original. That is, daughter particles carry a fraction z/z_0 of the originally large parent perpendicular momentum. Those that obtain a z near z_0 have a larger share than those which obtain a smaller z. It is this effect (combined with the fact that higher-z particles are more likely themselves to be primaries) which means that the higher-z particles ($z \gtrsim 0.1$) have a mean $k_\perp$ considerably larger than the average. (It is true that decay products with the very highest z/z_0 have received so much Q_z that the mean transverse decay momentum $Q_\perp$ must be smaller. But this depends on Q_z (or z/z_0) *via* a curve with a vertical tangent, an ellipse in fact, and the effect is not great and is overwhelmed by the $(z/z_0)p_\perp$ effect.)

The mean $k_\perp$ of all final particles is not much affected by the region $z \gtrsim 0.1$ because there are so many more particles of low z. Hence, the region $z \gtrsim 0.1$ can have a considerably higher $\langle k_\perp \rangle$ than the $\langle k_\perp \rangle$ of all particles. Far in the plateau of Y_z, one ultimately gets the same low mean of all particles. But, where the curve of the number of particles *versus* Y_z first begins to fall, the $\langle k_\perp \rangle$ begins to rise rapidly since each decay particle is sent to larger Y_z. For the true rapidity Y, however, decay sends particles equally up and down in Y so even a linear fall-off of the Y dis-

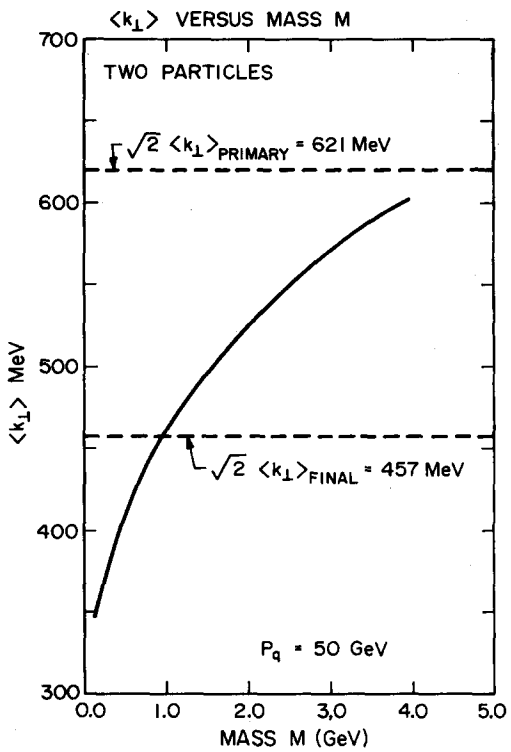

Fig. 34. The mean value of the transverse momentum, $\langle k_\perp \rangle$, of two particles *versus* the two-particle mass M. The results are for a u-quark of energy P_q = 50 GeV. Also shown, by dashed lines, is $\sqrt{2}$ times the $\langle k_\perp \rangle$ of primaries (621 MeV) and $\sqrt{2}$ times the $\langle k_\perp \rangle$ of the final mesons (457 MeV).

tribution would not distort the mean $k_\perp$. More radical variations, as those near the high Y_{end} do, however. The very highest Y values come from particles having abnormally low $m_\perp$ so the mean $k_\perp$ here is lower (see fig. 32).

Finally, for completeness, we show in fig. 34 the mean total $k_\perp$ of *two* particles whose mass M is given by

$$M^2 = (E_1 + E_2)^2 - (p_{z_1} + p_{z_2})^2 - k_\perp^2 \ , \tag{5.2a}$$

with

$$k_\perp^2 = (p_{x_1} + p_{x_2})^2 + (p_{y_1} + p_{y_2})^2 \ , \tag{5.2b}$$

where E_1 and E_2 are the energies of the two particles, respectively. As a function of the mass M, the two-particle $\langle k_\perp \rangle$ increases from a value of about 350 MeV at small mass M to a value equal to $\sqrt{2}$ times $\langle k_\perp \rangle_{\text{primary}}$ or about 621 MeV for M greater

than about 5.0 GeV. This sharp rise of $\langle k_\perp \rangle$ with mass M has also been observed in the plateau region of ordinary pp collisions [22].

We feel that the description of transverse momentum presented here is more satisfactory than the one used by us in FFF, in which all the final mesons in a quark jet had the same $\langle k_\perp \rangle_{q \to h} = 330$ MeV independent of z. We must change this to read that all *primary* mesons have the same $\langle k_\perp \rangle = 439$ MeV independent of z. Because the large-$p_\perp$ hadron experiments which we analyzed in FFF are sensitive predominantly to the large-z region of the quark decay functions so that $\langle k_\perp \rangle_{q \to h} \approx 439$ MeV, a number of our predictions in FFF will be changed *. For example, the mean values of P_{out} appearing in table 3 of FFF are all increased coming closer to the experimental findings. Also predictions made for experiments with small aperture acceptance will have to be reduced because of the wider spread in angle of the large-z particles. We are now computing corrections to FFF based on our new jet model. The results will be discussed elsewhere.

5.2. Correlations in transverse momentum

Our assumptions in subsect. 2.7.2 that each produced quark-antiquark pair conserves transverse momentum with no net $k_\perp$ and that the transverse momentum of a primary meson is the sum of the $k_\perp$ of two quarks leads to correlations in transverse momentum of the hadrons in the quark jet. As discussed in that subsection, primary mesons of adjacent rank tend to go oppositely with $\langle \boldsymbol{k}_{\perp_1} \cdot \boldsymbol{k}_{\perp_2} \rangle = -\sigma^2$. However, as we have already learned from fig. 22, adjacent-rank mesons can find themselves considerably spread apart in rapidity Y_z so that these correlations are of long range. Fig. 35 shows the behavior of the asymmetry

$$\Sigma(Y_1, Y_2) = [N_D(Y_2) - N_U(Y_2)] / [N_U(Y_2) + N_D(Y_2)], \tag{5.3}$$

where $N_U(Y_2)$ and $N_D(Y_2)$ are the number of hadrons at Y_2 with $|\phi_{12}| < \frac{1}{2}\pi$ and $|\phi_{12}| > \frac{1}{2}\pi$, respectively, and where ϕ_{12} is the angle between $\boldsymbol{k}_{\perp_1}$ and $\boldsymbol{k}_{\perp_2}$. This

* After the completion of FFF, in which we assumed $\langle k_\perp \rangle_{q \to h} = 330$ MeV independent of z, several people pointed out to us that there were indications that $\langle k_\perp \rangle$ was, in fact, larger than 330 MeV for large z both from hadron and lepton experiments. They further noted that we would improve our predictions of large-$p_\perp$ correlations in pp collisions if we took a larger $\langle k_\perp \rangle_{q \to h}$. In particular, we would predict a larger P-out in better agreement with experiment. It is now clear from the analysis of Seiden. [13] and from data on νp collisions [21,23] that $\langle k_\perp \rangle_{g \to h}$ *is* considerably larger than 330 MeV at large z. We have previously been reluctant to change (stubborn) because we did not want to "fiddle" our high-$p_\perp$ model in order to agree with the very experiments we were trying to predict. Now that we have added the physically natural assumption that some of the pions are secondary to resonances, we feel it is natural to replace the naive simple rule that the pions have a constant (with z) mean transverse momentum by the equally naive and simple rule that it is the *primaries* that have the constant transverse momenta. This, without further complication, leads to a natural explanation of many of the experimental observations. We shall adopt it hereafter. We are grateful to J. Vander Velde and Knud Hansen for discussions concerning this point.

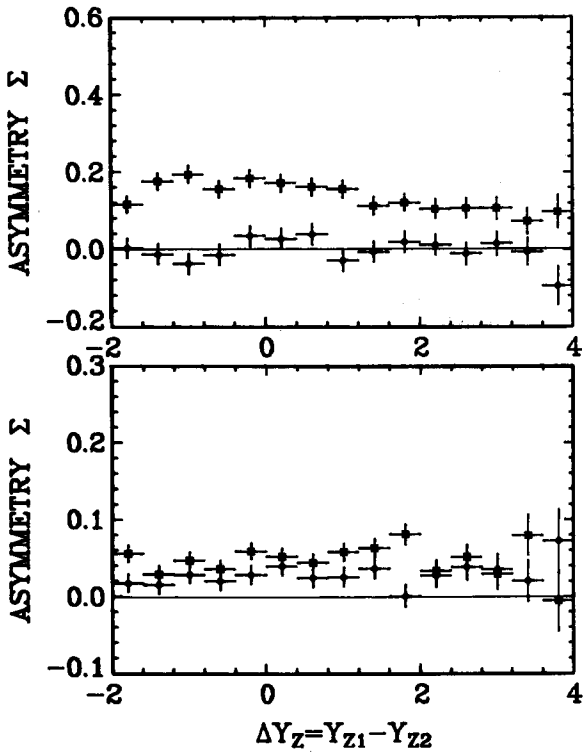

Fig. 35. Predicted behavior of the asymmetry $\Sigma(Y_1, Y_2) = (N_D(Y_2) - N_U(Y_2))/(N_U(Y_2) + N_D(Y_2))$ before (upper) and after (lower) decay of the primary mesons. The crosses (diamonds) are for the unlike (like) charge combinations and where N_U and N_D are the number of hadrons at Y_2 with $|\phi_{12}| < \frac{1}{2}\pi$ and $|\phi_{12}| > \frac{1}{2}\pi$, respectively, and ϕ_{12} is the angle between the transverse momentum vectors $k_{\perp_1}$ and $k_{\perp_2}$. The results are for particle h_1 at $Y_{z_1} = 4.0$ and are plotted *versus* $\Delta Y_z = Y_{z_1} - Y_{z_2}$. $a = 0.77$, $\alpha_{ps} = \alpha_v = 0.5$, $Y_{z_1} = (4.0, 4.4)$.

figure shows $\Sigma(Y_1, Y_2)$ for like and unlike charge combinations both before and after decay where particle one is at $Y_z = 4.0$ *versus* $\Delta Y_z = Y_{z_1} - Y_{z_2}$. (With this definition, Σ is positive for $k_{\perp_1} \cdot k_{\perp_2}$ negative.) Before decay, we see no correlation between same-sign mesons (since they cannot occur adjacent in rank) and a strong wide-range correlation between oppositely charged hadrons. Resonance decay plays a large role in determining the behavior of Σ. After decay, Σ is reduced for oppositely charged pairs and becomes non-zero and positive for same-sign hadrons. Similar transverse-momentum correlations have been observed in low-$p_\perp$ hadron-hadron collisions [24].

6. Some applications in large-$p_\perp$ hadron-hadron collisions

6.1. Large-$p_\perp$ particle ratios: comparison with FF1

Fig. 36 shows particle ratios for $\theta_{cm} = 90°$ pp collisions at large $p_\perp$ predicted using the quark-scattering model presented in FF1 but with our new quark-decay functions (analytic approximation). The quark-scattering model predicts that, except for the small smearing effects discussed in FFF, these ratios are functions only of $x_\perp = 2p_\perp/\sqrt{s}$ at fixed θ_{cm}. The new results are almost identical to those in FF1 except for the K^+/K^- ratio which is now somewhat larger (a factor of ≈ 1.8 at $x_\perp = 0.6$) due in part to (3.3). The new model, however, also allows us to investigate resonance production at large $p_\perp$. In fig. 37 predictions for ρ^0 (equal to ω^0) K^{*0}, $\bar{K}^{*0}$ and ϕ production are presented. (The ρ^0/π^0 ratio was constructed to approach one at large $x_\perp$ by our assumption that $\alpha_{ps} = \alpha_v$.) In addition, we calcu-

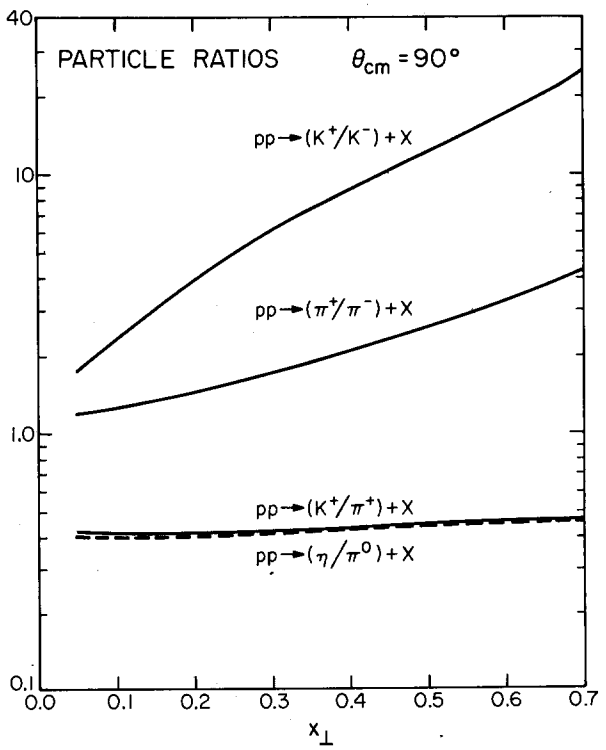

Fig. 36. Particle ratios *versus* $x_\perp = 2p_\perp/\sqrt{s}$ for $\theta_{cm} = 90°$ pp collisions at large $p_\perp$ predicted from the quark-scattering model of FF1 but using our new quark-decay functions.

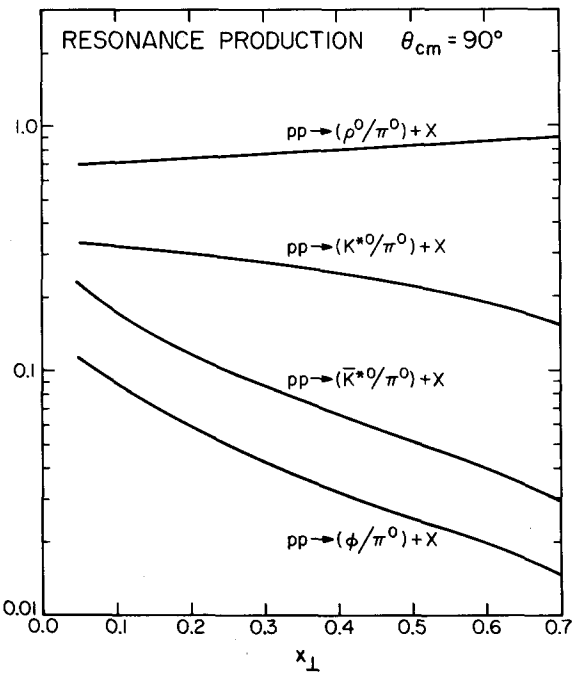

Fig. 37. Predicted ratios of resonance to π^0 production for $\theta_{cm} = 90°$ pp collisions *versus* $x_\perp = 2p_\perp/\sqrt{s}$ from the quark-scattering model of FF1 but using our new quark-decay functions.

Table 16
Comparison of large-$p_\perp$ particle ratios in pp collisions at $\theta_{cm} = 90°$ with the quark-scattering model of FF1 [4] using our new quark-decay functions, $D_q^h(z)$. Also shown are the contributions to the total π signal from ρ production and the contributions to the total K^+ signal from K^{*0} and ϕ production

Ratio	Experimental group	$x_\perp = 2p_\perp/\sqrt{s}$	Data	Predictions
π^+/π^-	C-P [28]	0.6	≃3.0	3.2
K^+/π^+	C-P	0.55	≃0.5	0.46
η/π^0	CCRS [29]	0.15	≃0.5	0.40
K^+/K^-	C-P	0.51	≃18	10.3
ρ^0/π^0	R-412 [30]	0.2	≃1.0	0.7
ϕ/π^0	C-F [31]	0.2	<0.06	0.06
$\rho^0 \to \pi^+/\pi^+$	R-410/13 [2,32]	0.1	≃0.05	0.08
$\rho^\pm \to \pi^0/\pi^0$	R-412	0.1–0.2	0.16	0.16
$K^{*0} \to K^+/K^+$	R-410/13	0.1–0.2	≃0.05	0.06
$\phi \to K^+/K^+$	R-410/13	0.1–0.2	0.005	0.01

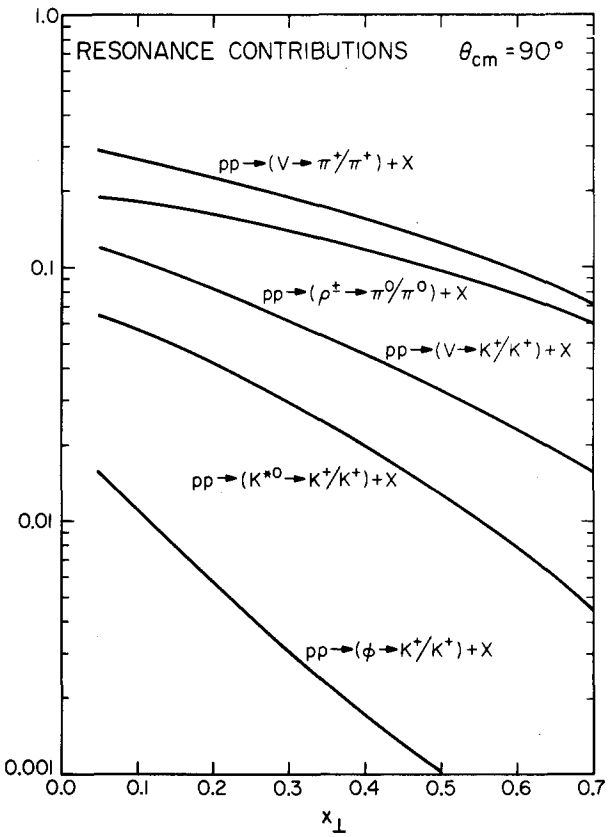

Fig. 38. Predicted contribution to the total large-$p_\perp$ meson signals for $\theta_{cm} = 90°$ pp collisions from resonance decays. The symbol V refers to the sum over all nine vector mesons and $K^{*0} \to K^+/K^+$ means the ratio of K^+'s due to K^{*0} decay to the *total* K^+ signal, etc.

late the fraction of the total large-$p_\perp$ signal that arises from the decay of various resonances. For example, fig. 38 shows that at ISR ($x_\perp = 0.1$) 27% of the total π^+ and 11% of the total K^+ signal comes from resonance decays. As $p_\perp$ increases, the contributions from resonance decays decrease. Table 16 gives a comparison of the expected values of various ratios with existing experimental data.

6.2. Same-side two-particle correlations: comparison with FFF ansatz

A distinctive feature of the quark-scattering model of FF1 is that high-$p_\perp$ particles in hadron-hadron collisions are not isolated but members of a cluster (jet) of particles representing the fragmentation of the quark. In FFF, we estimated the

number of particles to be found in the same direction as a large-$p_\perp$ trigger ("same-side" correlations) by assuming that the two-particle decay functions could be approximated in terms of the single-particle decay function by (FFF ansatz)

$$D_q^{h_1 h_2}(z_1, z_2) = D_q^{h_1}(z_1)\, D_{q_2}^{h_2}(z_2/(1-z_1))/(1-z_1)\,, \tag{6.1}$$

where h_1 is the trigger hadron so that $z_1 >> z_2$. The flavor of the quark q_2 was determined in the following manner. For what we called the "unambiguous" case where $h_1 = c\bar{a}$ contains the quark q, say q = c, then q_2 was taken to have the flavor "a". For example, if q is a u-quark and $h_1 = \pi^+$ or $h_1 = K^+$, then $q_2 = d$ or $q_2 = s$, respectively. For this case, we find the FFF ansatz to agree reasonably well with the results of our new jet model ($a = 0.77$ $\alpha_{ps} = \alpha_v = 0.5$).

On the other hand, we stated in FFF that (6.1) was not appropriate for the "ambiguous" case where h_1 does not contain the quark q as a valence quark. We find that indeed our new jet model disagrees quite substantially with the FFF ansatz for the "ambiguous" case. Since the predictions in FFF are dominated by the unambiguous case, we feel that they are reliable.

However, we can now use the new jet model to estimate the number of K^+'s produced in association with a large-$p_\perp$ K^- trigger in pp collisions, which we did not attempt in FFF because this is dominated by the "ambiguous" case, and to improve the other same side correlation estimates in FFF. Before this is done, however, we must also change our handling of the transverse momentum of the particles within the quark jet to agree with the results of subsect. 5.1. We expect to discuss this elsewhere.

7. Summary and conclusions

In summary, we have found that the recursive model gives a convenient and easy way to compute properties of a quark jet in terms of only a few parameters. Although the model does not include the possibility of baryon emission and cannot represent a true physical theory of jets; the resulting structure seems very reasonable and generally consistent with observations available so far. We recommend it as a "standard" jet to help design experiments and to which experiments may be compared and contrasted.

Aside from the mean number of particles (*versus* z), to which the model is fitted anyway, the main interesting feature is the distribution of charge, $D_q^{h^+}(z) - D_q^{h^-}(z)$, or of any other property by which jets originating from u-quarks can be distinguished from those from d-quarks. We can describe this as the distribution of the hadron containing the original quark. In the model, this is widely distributed. It is far from true that in an average (unbiased) jet the hadron of largest momentum always contains the original quark (see table 11). For jets of limited momentum, individual d-quark jet events can often look just like u-quark events and a reliable way to distinguish them

event-by-event seems unavailable. They can, of course, be distinguished by their average properties. But our model, just like experiment, finds large statistical variations from event to event so that good averages require many events. (This can be seen most clearly on many of the Monte Carlo plots. Even for 40 000 jets, there are uncomfortably wide fluctuations for many quantities of interest.) One of the first things to determine experimentally is whether $D_q^{h^+}(z) - D_q^{h^-}(z)$ is really as widely distributed (see figs. 5, 8, and 12) as our model (or the previous parametrization of FF1) suggests. Preliminary experimental indications are that it is [15,21,23].

The hadrons observed in quark jets can be secondaries from the decay of higher resonances (we have included only the 1^- vector resonances). Although the model makes interesting special predictions for how these *primaries* may be correlated, we find the correlations are spread widely in rapidity, and are further considerably obscured by the correlations induced by resonance decay. This makes it hard to check the specifies of the recursive idea, but it helps us in our original purpose; to generate a standard jet that ought to look much like nature.

From our experience, we think that different jet models which have the right mean distributions of the various hadrons and which include the production of resonances in a way roughly consistent with experiment (our precise choice $\alpha_v = \alpha_{ps} = 0.5$ may require later modification) will be very difficult to distinguish experimentally. The recursive scheme is as good as any for our purpose *.

This is well illustrated by transverse-momentum distributions. Many interesting variations which have been observed (*versus* z or the two-particle mass M) in lepton and hadron experiments appear to be merely consequences of the fact that hadrons are often secondaries of primaries with much simpler properties. In fact, the primaries might all have a uniform transverse-momentum distribution.

For these reasons, we think of our jet model, not as an interesting theory to be checked by experiment, but rather as a possibly reliable guide as to what general properties might be expected experimentally. In particular, it can assist in the program of comparing hadron high-$p_\perp$ jets to lepton-generated jets.

On the other hand, quark jets are often investigated not just to be used as a tool to investigate hadron collisions, but rather as a subject of interest in itself. How are quark jets actually generated? From what we have learned, we think it will tax the ingenuity of experimenters to see behind those properties which are overshadowed by the effects of resonance decay in order to study effects more intrinsically related to the process of jet formation.

In this connection, the most fundamental experimental question is whether lepton-induced jets really have a quark origin at all. Even here we find difficulties. Properties averaged over many jets are unconvincing, for a *mean* charge, say, of $\frac{2}{3}$ can be achieved by averaging over events each of which is associated with an integral charge. The most promising method would seem to be the momentum weighted charge $Q_W(p)$ in (3.9). In principle, at least, for a jet of sufficiently large momentum, this

* For examples of other jet models see refs. [13,25–27].

is a characteristic of the object generating the jet and one which can be checked for each event separately. Unfortunately, in practice, it will be difficult to use for even 10 GeV jets (see fig. 21), if the charge is spread as widely as in our model. The method improves, but only slowly, as the jet energy increases.

We are grateful to C. Bromberg, G. Fox, and C. Quigg for numerous informative discussions. Also, we thank T. Ferbel, K. Hanson and J. Vander Velde for useful correspondence.

Note added in proof

It has been suggested to us that perhaps the simple form for $f(\eta)$ in (2.21) that we have used results in a distribution of quark charge, $D_q^{h^+}(z) - D_q^{h^-}(z)$, that is broader than actually implied by the fit to $D_u^{h^+}(z) + D_u^{h^-}(z)$ in fig. 3. For example, a form like $f(\eta) = A(1-\eta)^n\,(1 - a + 3a\eta^2)$ (normalized properly) would produce a quark charge that is isolated more toward the end of the quark (high z). Such a form produces a $zF(z)$ that tends to dip at small z, but this possibility cannot be ruled out since the data in fig. 3 cannot be used for $z \lesssim 0.3$. Hence one can view our jet model as a bit pessimistic. It results in a widely distributed quark charge and an order in rapidity and hierarchy that is quite mixed up. We must ultimately resort to experiment to see if $D_u^{h^+}(z) - D_u^{h^-}(z)$ is as widely distributed as our model suggests.

References

[1] D. Linglin, Observation of large-$p_\perp$ jets at the ISR and the problem of parton transverse momentum, Invited talk at 12th Rencontre de Moriond, March 1977.
[2] R. Moller, Jets and quantum numbers in the high-$p_\perp$ hadronic reactions at the CERN ISR, Invited talk at 12th Rencontre de Moriond, March 1977.
[3] C. Bromberg et al., Phys. Rev. Lett. 38 (1977) 1447;
E. Malamud, Comparison of hadron jets produced by π^- and p beams on hydrogen and aluminum targets, Invited talk presented at 8th Int. Symp. on multiparticle dynamics, Kaysersberg, France, June 1977.
[4] (FF1) R.D. Field and R.P. Feynman, Phys. Rev. D15 (1977) 2590.
[5] (FFF) R.P. Feynman, R.D. Field and G.C. Fox, Nucl. Phys. B128 (1977)1.
[6] A. Krzywicki and B. Petersson, Phys. Rev. D6 (1972) 924.
[7] J. Finkelstein and R.D. Peccei, Phys. Rev. D6 (1972) 2606.
[8] J.D. Bjorken, High-$p_\perp$ dynamics, Lecture given at SLAC Summer Institute on particle physics, November 1975.
[9] S.D. Ellis, M. Jacob and P.V. Landshoff, Nucl. Phys. B108 (1976) 93.
[10] A. Casher, J. Kogut and L. Susskind, Phys. Rev. Lett. 31 (1973) 792.
[11] G.R. Farrar and J.L. Rosner, Phys. Rev. D9 (1974) 2226.
[12] R.N. Cahn and E.W. Colglazier, Phys. Rev. D9 (1974) 2658.
[13] A. Seiden, Phys. Lett. 68B (1977) 157; Hadron distributions in a quark-parton model, SLAC-PUB-1962, Nucl. Phys. B, submitted.

[14] R.P. Feynman, Photon-hadron interactions (Benjamin, Reading, Mass., 1972).
[15] J.C. Vander Velde, Berkeley-Fermilab-Hawaii-Michigan Collaboration, Neutrino-proton interactions in the 15-Foot Bubble Chamber and properties of hadron jets, Invited talk presented at 4th Int. Winter Meeting on fundamental physics, Salardú, Spain, 1976.
[16] P. Pirilä, G.H. Thomas and C. Quigg, Phys. Rev. D12 (1975) 92;
C. Quigg, P. Pirilä and G.H. Thomas, Phys. Rev. Lett. 34 (1974) 290;
A. Krzywicki and D. Weingarten, Phys. Lett. 50B (1974) 265.
[17] C. Quigg, What have we learned from high-energy experiments?, Invited talk presented at the 1973 APS/DPF Meeting in Berkeley, AIP Proc. No. 14, subseries no. 6.
[18] E.L. Berger, Phys. Lett. 49B (1974) 369.
[19] T. Ferbel, Recent results from bubble-chamber experiments at Fermilab, invited talk at the SLAC Summer Institute on particle physics, SLAC report No. 179 (1974).
[20] S.J. Brodsky and J.F. Gunion, Hadronic fragmentation as a probe of the underlying dynamics of hadron collisions, UCD-77-9, SLAC-PUB-1939, Phys. Rev., to be published.
[21] M. Derrick et al., Properties of the hadronic system resulting from $\bar{\nu}p$ interactions, ANL-HEP-PR-77-39, Phys. Rev. D, submitted.
[22] P. Stix et al., Transverse-momentum properties of multi-pion systems produced in high-energy collisions, Univ. of Rochester preprint UR-611.
[23] J.C. Vander Velde, Berkeley-Fermilab-Hawaii-Michigan Collaboration, Neutrino interactions in the 15-Foot Hydrogen Bubble Chamber and search for charmed particles, Invited talk presented at 12th Rencontre de Moriond, Flane, France 1977.
[24] C. Bromberg et al., Phys. Rev. D10 (1974) 3100.
[25] H. Fukuda and C. Iso, Prog. Theor. Phys. 57 (1977) 483.
[26] O. Sawada, Quark-cascade model; hadronization of quarks after a hard collision, Tohoku University preprint TU/77/166, 1977.
[27] U.P. Sukhatme, Quark jets: a quantitative description, University of Cambridge preprint, DAMTP 77/25.
[28] H. Frisch, A review of high transverse momentum processes, Invited talk at APS meeting, Brookhaven, October 1976;
D. Antreasyan et al., Chicago-Princeton preprint CP76-2.
[29] F.W. Busser et al., Phys. Lett. 55B (1975) 232.
[30] D. Darriulat et al., Nucl. Phys. B107 (1976) 429.
[31] J.A. Appel et al., Phys. Rev. Lett. 35 (1975) 9
[32] H. Bøggild, Event structures in large-$p_\perp$ hadron-hadron collisions, Invited talk given at 8th Int. Symp. on multiparticle dynamics, Kaysersberg, France, 1977.